Lawrence Berkeley Laboratory
UNIVERSITY OF CALIFORNIA

Materials & Molecular Research Division

Submitted to Proceedings of the IEEE

ADVANCES IN SQUID MAGNETOMETERS

John Clarke

June 1980

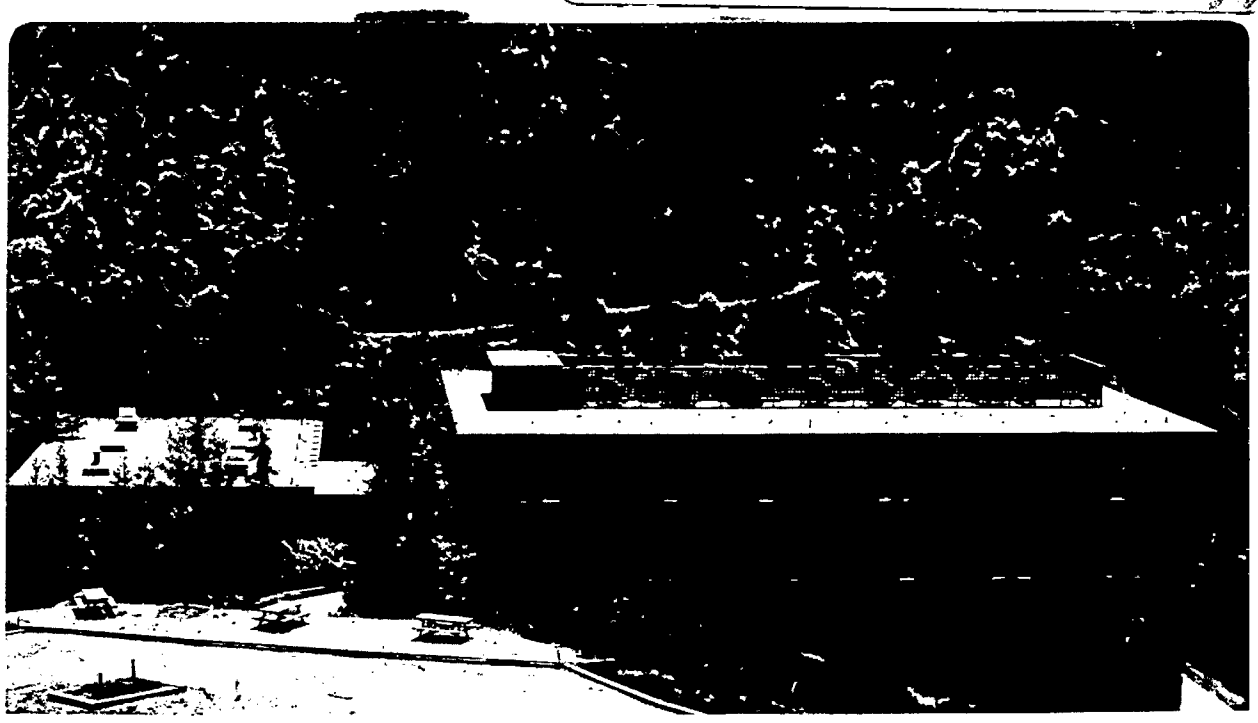

Prepared for the U.S. Department of Energy under Contract W-7405-ENG-48

DISCLAIMER

To be Published in Proc. IEEE

LBL 10845

Advances in SQUID Magnetometers

John Clarke

Invited Paper

Abstract -- The operation and noise limitations of dc and rf SQUIDs are outlined, and recent advances in their sensitivity are discussed. A model of the dc SQUID predicts an energy noise level per Hz referred to the SQUID of approximately $8\ k_B T\ L/R \approx 8\ k_B T(\pi LC)^{\frac{1}{2}}$, where L, R, and C are the SQUID inductance and the shunt resistance and capacitance of each Josephson junction. Some examples of dc SQUIDS are described to show that their performance is generally in reasonable agreement with the model. The noise energy has improved from about 2×10^{-30} JHz^{-1} for a device with L=1nH and a tunnel junction area of 10^4 μm^2 to about 2×10^{-33} JHz^{-1} for a device with L=0.1nH and a microbridge resistance of 40 Ω. Further improvements are expected in the near future. The model of the rf SQUID predicts a noise energy per Hz referred to the SQUID of $[(\pi\alpha^2\phi_0^2/2L) + 2\pi\alpha k_B T_a^{(eff)}]/\omega_{rf}$, where α is the intrinsic width of the distribution of flux transitions, $T_a^{(eff)}$ is an effective amplifier noise temperature, and ω_{rf} is the pump frequency.

With one exception, the performance of the 7 types of rf SQUID listed is in reasonable agreement with the model. The noise energy ranges from about 1.5×10^{-29} JHz^{-1} for a 20 MHz toroidal SQUID to 3.5×10^{-31} JHz^{-1} for 9 GHz re-entrant toroidal SQUID; a somewhat better sensitivity has been reported for a 430MHz device, /apparently in conflict with the theory. In both dc and rf SQUIDS, 1/f noise (f is frequency) is likely to extend to higher frequencies as the white noise level is decreased.

Manuscript received March , 1980. This work was supported by the Division of Materials Sciences, Office of Basic Energy Sciences, U.S. Department of Energy.

The author is with the Department of Physics, University of California and Materials and Molecular Research Division, Lawrence Berkeley Laboratory, University of California, Berkeley, California 94720.

I. INTRODUCTION

During the past two years, the energy sensitivity of dc SQUIDs (Superconducting QUantum Interference Devices) [1] has improved by more than 3 orders of magnitude, while that of rf SQUIDs [2,3] has improved by perhaps an order of magnitude. The purpose of this article is to review briefly these advances, and to make some assessment of possible future trends.

A few general remarks on the history of SQUIDs are in order. The dc SQUID, which consists of two Josephson junctions [4] interrupting a superconducting loop, appeared in 1964. The critical current (maximum supercurrent) of the SQUID oscillates as a function of the flux, ϕ, threading the ring with a period of one flux quantum. When the SQUID is biased with a constant current, the time-averaged voltage is also periodic in ϕ, so that the SQUID is essentially a flux-to-voltage transducer. The potential of the device as a sensitive magnetometer and voltmeter was immediately recognized, and several versions were made and used. Ironically, although the first dc SQUID was fabricated from thin films [1], the early practical devices were made from niobium block, sheet, or wire. Development of the dc SQUID was largely abandoned around 1970 because of the advent of the rf SQUID, which requires only a single junction to be mounted in the loop. The rf SQUID is coupled to the inductor of a resonant LC- circuit, excited at its' resonant frequency. The rf voltage across the tank circuit is also periodic in the flux in the SQUID. At a time when reproducible, stable junctions were relatively difficult to produce, the rf SQUID had an obvious advantage in simplicity over the dc SQUID. Subsequently, there was considerable activity in the development of rf SQUIDs, their associated electronics, and the theory of their noise limitations. Most devices involved a niobium point contact, although some thin-film microbridge versions were also used successfully. Several companies manufactured rf SQUIDs,

particularly toroidal point contact devices,
and they have become very much more widespread in applications than the dc SQUID. However, in 1974, a cylindrical thin-film tunnel junction dc SQUID appeared with a sensitivity substantially higher than that of available rf devices. It was long-lived, relatively easy to fabricate, and required quite simple electronics. A model for the noise predicted that one could hope to improve on the sensitivity of the 1974 SQUID by between 3 and 4 orders of magnitude. These improvements have now been largely realized, and the sensitivity of the SQUID is approaching a quantum/mechanical limit. Thus, although rf SQUIDs are still by far the more popular, it appears that dc SQUIDs may well return to favor in the near future.

In this article, I shall discuss recent developments in dc and rf SQUIDs, beginning in each case by discussing briefly the principles of their operation, their noise limitations, and the optimization of their sensitivity. I shall then describe a number of devices, and compare their sensitivities with the predictions of the models. The list of devices is not intended to be exhaustive: It was chosen to illustrate improvements in the sensitivity of dc SQUIDS over the cylindrical device, and in the sensitivty of rf SQUIDS over the toroidal device. I shall not be concerned with other important considerations, such as the slewing rate, which is largely a function of the associated electronics, or the input circuitry required for voltmeters or magnetometers. Extensive references and details of early work, the theory of SQUID operation, and a discussion of input circuits can be found in earlier reviews [5, 6].

II. DC SQUID

A. Principles of Operation

The dc SQUID consists of two Josephson junctions in a superconducting loop of inductance L [Fig. 1(a)]. We assume that the junctions are ideal tunnel junctions each with a critical current I_0 and a self-capacitance C. Each junction is resistively shunted to eliminate hysteresis on the current-voltage (I-V) characteristic. This requires [7] $\beta_c = 2\pi I_0 CR^2/\phi_0 \lesssim 1$, where $\phi_0 = h/2e$ is the flux quantum. Figure 1(b) shows the I-V characteristics of the device with applied fluxes $\phi = n\phi_0$ and $(n + \frac{1}{2})\phi_0$ threading the loop, where n is an integer. The critical current of the SQUID oscillates as a function of ϕ. The I-V characteristic is also a periodic function of ϕ, so that if one biases the SQUID with a constant current greater than the maximum critical current, the voltage across the device is as indicated in Fig. 1(c). For a flux near $(2n + 1)\phi_0/4$, the SQUID is thus a flux-to-voltage transducer with a transfer function $V_\phi \equiv (\partial V/\partial \phi)_I$. The equivalent flux sensitivity of the device is determined by dividing the rms voltage noise across the SQUID by V_ϕ to obtain the equivalent rms flux noise.

In practice, SQUIDs are almost invariably operated in a flux-locked loop as indicated in Fig. 2. An ac flux (typically at 100kHz) with peak-to-peak amplitude $\phi_0/2$ is applied to the SQUID, and the resultant 100kHz voltage is amplified by either a cooled LC- resonant circuit [8] or a cooled transformer [9]. If the average flux in the SQUID is exactly $n\phi_0$ [Fig. 3(a)], the voltage across the SQUID is at 200kHz. If the flux is increased or decreased from this value, a 100kHz component appears in the voltage, with a phase that depends on the sign of the flux change [Fig. 3(b)]. The 100kHz signal is amplified and lock-in detected at the modulation frequency, as indicated in Fig. 2.

Thus, the output from the lock-in is zero at $n\phi_0$, positive (say) for $\phi = (n+\delta)\phi_0$, and negative for $\phi = (n-\delta)\phi_0$, where $\delta << 1$. After further amplification, the voltage is connected across a resistor in series with the modulation/feedback coil coupled to the SQUID. Thus, if a flux $\delta\phi_0$ is applied to the SQUID, the feedback current produces an opposing flux that cancels $\delta\phi_0$, the output voltage V_0 being proportional to $\delta\phi_0$.

To measure the intrinsic equivalent flux noise of the SQUID, the device is enclosed in a superconducting shield to exclude fluctuations in the external magnetic field. The spectral density of the noise in the output is measured, and can be converted readily into an equivalent flux noise provided the feedback resistance, R_F, and the mutual inductance between the feedback coil and the SQUID are known.

B. Noise and Optimization

Tesche and Clarke [10] have performed a computer simulation of the dc SQUID to find the optimum parameters, assuming that the only source of noise is Nyquist noise in the resistive shunts. They computed the I-V characteristics and noise with zero junction capacitance. To compare their model with a real SQUID with non-zero capacitance they used the maximum value of resistance for non-hysteric behavior, $R = (\phi_0/2\pi I_0 C)^{1/2}$. The presence of capacitance undoubtedly affects both V_ϕ and the level of the voltage noise, but it is believed that the error introduced into the computed energy noise is at most a factor of 2. The simulation confirmed the long-held belief that the SQUID is optimized when $\beta = 2LI_0/\phi_0 \doteq 1$. Most of the computations were performed for a SQUID operating in the liquid He^4 range with L=1nH and I_0=1μA. The choices of I_0 and the temperature T fix the noise parameter $\Gamma = 2\pi k_B T/I_0 \phi_0$ to be about 0.05 at 1.2K. This parameter determines the noise rounding of the I-V characteristic as well as the magnitude of the noise, and its' value can drastically affect the value of V_ϕ. Thus, computations at a given value of Γ cannot be applied immediately

to devices with very different values of Γ. There is a peak in V_ϕ as a function of bias current, and it is necessary to operate the SQUID at or close to this peak to obtain optimum performance. For L=1nH, I_o=1μA, and Γ= 0.05, to a good approximation the optimum value of V_ϕ at $\phi \approx (2n+1)\phi_o/4$ is

$$\left(\frac{\partial V}{\partial \phi}\right)_I \approx \frac{R}{L} . \tag{1}$$

The spectral density, S_V, of the voltage noise across the SQUID at frequencies much less than 2eV/h (but greater than frequencies at which 1/f noise appears, where f is the frequency) is white, proportional to Γ, and modulated somewhat with the flux with a period ϕ_o. For the same values of L, I_o, and Γ given above, or $\phi = (2n+1)\phi_o/4$, and at the peak in V_ϕ, S_V has the value

$$S_V \approx 16\, k_B T R. \tag{2}$$

Bearing in mind that the resistance of the SQUID at high bias currents is R/2, we notice that the spectral density of the voltage noise at the operating point is roughly 8 times the Nyquist value for the shunt resistances. Combining Eqs. (1) and (2) we find the <u>equivalent</u> flux noise:

$$S_\phi \approx 16\, k_B T\, L^2/R . \tag{3}$$

For many practical applications in which the SQUID is coupled to an input circuit to make a voltmeter or magnetometer, it is important to realize that a knowledge of S_ϕ is <u>not</u> necessarily sufficient to characterize the sensitivity of the device. In addition to the voltage noise across the SQUID there is a noise current circulating around the SQUID loop. For the same values of L, I_o, Γ, and ϕ used above, and at the peak in V_ϕ, the computer model predicts the spectral density of the current noise to be [12]

$$S_J \approx 11\, k_B T/R. \tag{4}$$

Whether or not there is an input circuit coupled to the SQUID, the current noise gives rise to a component of the voltage noise provided $V_\phi \neq 0$. The voltage and current noises are therefore partially correlated, and have a

correlation power spectral density [12]

$$S_{VJ} \approx 12\, k_B T \tag{5}$$

for the above values of L, I_o, Γ and ϕ. The circulating current noise also induces a real voltage noise in any input circuit coupled to the SQUID that is detected and amplified by the SQUID to produce an additional voltage noise at the SQUID output. The optimization of voltmeters and magnetometers taking into account these two noise sources is relatively straightforward [13], and we shall briefly discuss the results for voltmeters with tuned and untuned input circuits, as indicated in Fig. 4.

For a tuned voltmeter [Fig. 4(a)], when the components have been properly optimized for a signal frequency $\omega \ll R/L$, the optimum noise temperature (Eqs. (15) and (16) of ref. [13]) is

$$T_N^{(opt)} \approx \frac{\omega}{2k_B V_\phi} (S_V S_J - S_{VJ}^2)^{\frac{1}{2}}. \tag{6}$$

Notice that $T_N^{(opt)}$ is independent of the coupling coefficient between the input circuit and the SQUID, and is reduced by the correlations in the two noise sources. Both $S_V S_J$ and S_{VJ}^2 are proportional to $(k_B T)^2$, and

$$T_N^{(opt)} \approx \frac{\omega}{\sqrt{8}\, k_B} \frac{S_\phi}{2L} \approx \frac{\sqrt{8}\,\omega T}{R/L}. \tag{7}$$

For the untuned voltmeter [Fig. 4(b)], the optimized noise temperature (Eqs. (17) and (18) of ref. [13]) for $\omega \ll R/L$ is

$$T_N^{(opt)} = \frac{\omega S_V}{2k_B \kappa^2 V_\phi^2 L} \left[1 + \left(\frac{2\kappa^2 S_{VJ} V_\phi L}{S_V} + \frac{\kappa^4 V_\phi^2 R^4 S_J}{L^2 S_V}\right)\right]^{\frac{1}{2}}. \tag{8}$$

Here $\kappa = M_i/(L L_i)^{\frac{1}{2}}$ is the coupling coefficient between the input coil and the SQUID, and M_i is the mutual inductance between the SQUID and the input coil of inductance L_i. Setting $S_\phi = S_V/V_\phi^2$, and neglecting the

term in square brackets which lies between 1 and 2, we find

$$T_N^{(opt)} \gtrsim \frac{\omega S_\phi}{2k_B\kappa^2 L} - \gtrsim \frac{8\,\omega T}{\kappa^2 R/L} \quad . \tag{9}$$

Unfortunately, no measurements exist for either S_J or S_{VJ}. However, to the extent that one has faith in the model, it is clear that if one designs a SQUID to optimize $S_\phi/2L$ by maximizing R/L, the noise temperature will also be minimized. A convenient parameter for characterizing SQUIDs is thus the noise energy per Hz

$$\varepsilon/1\text{Hz} = S_\phi/2L \quad . \tag{10}$$

From Eq. (3), we find

$$\varepsilon/1\text{Hz} \gtrsim 8k_BT/(R/L), \tag{11}$$

or, setting $R = (\phi_o/2\pi I_o C)^{\frac{1}{2}}$ and $2LI_o = \phi_o$,

$$\varepsilon/1\text{Hz} \gtrsim 8k_BT(\pi LC)^{\frac{1}{2}} \quad . \tag{12}$$

It should be emphasized that the numerical factor in Eqs. (11) and (12) is somewhat dependent on the value of Γ used in the calculation, 0.05, and is likely to be substantially different for much larger or much smaller values of Γ. Nevertheless, the functional dependences are valid for all situations in which thermal noise in the shunts is the only, or at least the dominant noise source. Thus, to optimize the SQUID we must reduce T, L, and C. Since the capacitance of a tunnel junction changes relatively little as the critical current is varied over a wide range, a reduction in C is equivalent to a reduction in the junction area. A reduction in C increases the bias voltage and hence the Josephson frequency at which the SQUID operates, and is thus analogous to increasing the pump frequency of the rf SQUID. We also point out that Eqs. (11) and (12) neglect preamplifier noise. It is relatively straightforward to obtain a preamplifier noise temperature rather less than 1K so that this noise contribution is insignificant for a SQUID in the He^4 temperature range. However, if the temperature were to be lowered into the mK range, one would require a preamplifier

with a lower noise temperature (for example, a second SQUID,) to take advantage of the reduced intrinsic thermal noise. As a final comment on the noise energy we note that in most low frequency applications one uses an untuned rather than a tuned input circuit. The noise energy is then proportional to $1/\kappa^2$, so that $\varepsilon/1\text{Hz} = S_\phi/2L\kappa^2$ is a more appropriate parameter to compare different SQUIDs. As we shall see, most of the very sensitive devices recently produced have not been coupled to input circuits, and the value of κ obtainable remains an open question. We shall therefore use Eq. (10) as a measure of the sensitivity, but one should bear in mind its' limitations.

Our discussion so far has been for noise in the thermal limit. However, if one can design and fabricate a SQUID such that the bias voltage at the peak in V_ϕ exceeds k_BT/e, quantum effects will become important. Calculations by Koch et al. [14] suggest that in the limit $eI_oR >> k_BT$, the sensitivity is limited by zero point fluctuations in the shunt resistors. At T=0, for an optimized tuned input circuit they find $\varepsilon/1\text{Hz} \approx \hbar$, and $T_N^{(opt)} \approx \hbar\omega/k_B$. These results may be understood qualitatively if one replaces k_BT with eI_oR in Eqs. (11) and (7), and $/2LI_o = \phi_o$. At the time of writing, it seems possible to operate a dc SQUID in the quantum noise limit.

In section II.C we describe a number of practical SQUIDs that have been designed for low noise according to the prescription in this section. Although there are deviations in detail from the equations given for the thermal noise limit, these results appear to be reasonably accurate, and to provide an excellent guideline for the optimization of SQUID parameters.

C. Practical Thin-film dc SQUIDs

Six types of dc SQUID are described. The essential parameters are summarized in Table I, with values of $S_\phi/2L$ predicted from Eq. (11).

(i) Cylindrical dc SQUID with L=1nH and $10^4 \mu m^2$ junctions The first practical thin-film tunnel junction SQUID was the cylindrical device [8] shown in Fig. 5. The various metals are deposited through shadow masks onto a 3mm diameter fused quartz tube. The Nb strips make metallic contact with the Pb(10% In) band, and are thermally oxidized before the two junctions are completed by the evaporation of the Pb/In tee. Each junction has an estimated capacitance of about 400pF, and a critical current of 1 to 2 μA. The Au strip, which is deposited first, provides a shunt resistance of about 1Ω for each junction. Thus, β_c is usually between 1 and 2, but no hysteresis in the I-V characteristic is observed because of noise rounding. The sensor is covered with a thin insulating layer, and a lead film is evaporated over the slit in the band and the narrow films. This superconducting groundplane substantially reduces the parasitic inductance. The total SQUID inductance is approximately 1nH, and β varies from 1 to 2. The modulation/feedback coil, typically 2 turns of 50μm-diameter niobium wire, is mounted rigidly inside the quartz tube, while the signal coil is wound on a cylindrical former that fits snugly over the SQUID. The cylindrical configuration enables one to achieve excellent magnetic coupling between the signal coil and the SQUID. A coupling coefficient, κ, of 0.5 to 0.6 is typical. Two leads are connected to the SQUID with pressed In pellets.

The spectral density of the flux noise with the SQUID in a flux-locked loop is typically $10^{-9}\phi_o^2$ Hz^{-1} at frequencies above about 2 X 10^{-2} Hz, corresponding to an energy noise of about 2×10^{-30} JHz^{-1}. At lower frequencies 1/f noise dominates. These devices have been in use for about 6 years, and have proved to be completely reliable even under the demanding conditions of geophysical field trips. They are rather insensitive to the exact values

of the ac modulation amplitude and bias current, so that one does not usually need to make any adjustments during trips lasting as long as several weeks. Furthermore, because the critical current is relatively insensitive to bath temperature, it is usually not necessary to adjust the bias when the magnetometer is operated at higher altitudes.

(ii) Planar dc SQUID with L=1nH and $10^2\mu m^2$ junctions To test the effects of reducing the junction capacitance, Koch et al. [15] have constructed planar SQUIDs with an inductance of 1nH and a junction area of $10^2\mu m^2$, thereby reducing the capacitance to about 4 pF. The SQUIDs are constructed by first evaporating two 10μm-wide AuCu shunts through shadow masks (Fig. 6), and then sputtering a Nb loop in the configuration shown using a photolithographic lift-off technique. The surface of the Nb is cleaned by ion-milling and thermally oxidized before the final Pb/In film is deposited through a shadow mask. The modulation/feedback coil is glued to the substrate near the SQUID loop. Above roughly 1Hz, the noise energy of an optimum device in an open loop measurement is $2\times10^{-31}JHz^{-1}$, in good agreement with the expected value.

(iii) Planar dc SQUID with n=1nH and $1\mu m^2$ junctions Voss et al. [16] have constructed an all-Nb planar device with $1\mu m^2$ junctions that has the expected performance, and that is particularly durable. The SQUIDs are fabricated on 33μm-thick Si wafers using electron beam lithography (Fig. 7). The shunt resistors are made by depositing 20nm of Pd, lifting-off the mask, and annealing the substrate at 250°C for 30 min. to form Pd_2Si. The resistivity of this material varies from 40 to 80 μΩ cm. A second resist layer is patterned for the first Nb film with a 1μm linewidth in the regions where the junctions are to be formed. After plasma etching the exposed substrate, a 135nm-thick Nb film is deposited and the mask lifted off. A final resist layer is patterned for the second Nb film to give linewidths at the junctions of between 0.5 and 4μm. The exposed first Nb film is sputter-cleaned and plasma ozidized before the deposition of a 210nm-thick Nb film. After the final lift-off, the wafer

is diced, and Al wires are ultrasonically bonded to the Nb pads. The estimated inductance of the SQUID is 1nH.

Figure 8 shows the I-V characteristics at two temperatures with applied fluxes of $n\phi_0$ and $(n+\frac{1}{2})\phi_0$. There is no evidence of resonant structure on the characteristics. The resistance of the SQUID at high bias current is 15Ω, corresponding to a shunt resistance of 30Ω for each junction. Figure 9 shows $V(\phi)$, V_ϕ, V_n (rms voltage noise), ϕ_n (rms flux noise), and ε/1Hz vs. applied flux. The bias current was adjusted to maximize the change in $V(\phi)$ with flux, and the noise was measured at 40kHz. The maxima of V_ϕ and V_n and the minima of ϕ_n and ε all occur at the same values of applied flux. At 1.6K, an optimum energy noise of 1.1×10^{-32} J Hz^{-1} was obtained over a variation of applied flux of at least $\phi_0/10$, and at bias currents of 3.7 ± 0.2μA. At 4.2K, the energy noise of 2.5×10^{-32} JHz^{-1} was similarly insensitive to the bias current, and achieved over a range of $\phi_0/10$ or more. Thus, there should be no difficulty in operating the device in a flux-locked loop. This type of SQUID appears to be virtually indestructible and, coupled efficiently to a suitable input coil, it would make an exceedingly useful general purpose device.

(iv) Planar dc SQUID with L=11.5pH and 10μm^2 junctions An alternative way of improving the noise energy of the dc SQUID is to reduce its' inductance, although this may make the device more difficult to couple efficiently to an external coil. Ketchen and Voss [17] have constructed the SQUID shown in Fig. 10 with an inductance of about 11.5pH and a junction area of 10μm^2. The SQUID was fabricated on a superconducting groundplane to lower the loop inductance, using the standard IBM Pb-alloy process for fabricating computer circuits [18]. In contrast to the all-Nb SQUID described above, the I-V characteristic of the low-inductance SQUID showed considerable structure, presumably due to standing-wave modes in the device.

The resistance per shunt was about 2Ω. The transfer function V_ϕ has two peaks of about 4mV ϕ_0^{-1} that are separated by about $0.6\phi_0$, while the noise voltage has two small peaks corresponding to the two large peaks in V_ϕ, and a third large peak corresponding to a small peak in V_ϕ. The values of ϕ_n and ε show correspondingly sharp minima. The optimum value of ε/1Hz is about 3×10^{-33} J Hz^{-1} or about 5h. When the SQUID was cooled to 1.8K, both V_ϕ and V_n increased, but the optimum value of ε remained at 5h over an even shorter range in ϕ, about $\phi_0/200$. It appears that the high sensitivity was obtained at a bias current where the dynamic resistance was extremely high. Because V_ϕ is close to zero at this bias current for most values of applied flux, and because the peaks in V_ϕ are not separated by exactly $\phi_0/2$, it may be difficult to flux-modulate and operate this SQUID in a flux-locked loop in the usual way. The fact that ε did not improve when the SQUID was cooled is somewhat puzzling, since the sensitivity still appears to be well above the quantum limit. Nevertheless, it is noteworthy that the SQUID showed such impressive sensitivity despite the rather pathological dependence on flux, since it implies that a high degree of symmetry in V vs. ϕ is not essential for high sensitivity [10].

(v) Planar dc SQUID with L=0.2nH and 3μm^2 junctions with Ge-Sn barriers Hu et al. [19] have described a technique for fabricating Pb-GeSn-Sn junctions. The GeSn barrier is typically 50nm-thick, and has a sufficiently low capacitance that junctions with current densities of 10^3A cm^{-2} or higher have non-hysteretic I-V characteristics without the need for external shunts. These junctions have been incorporated into a planar SQUID with L ≈ 0.2nH, and R ≈ 40Ω per junction. At 2K, the measured energy sensitivity was about 10^{-31} J Hz^{-1} at frequencies above the 1/f region. It appears that the sensitivity

was limited by amplifier noise rather than intrinsic SQUID noise, since no cooled matching circuit was used: The value of $V_\phi \approx 300\mu V\ \phi_o^{-1}$ together with an amplifier noise of $\sim 1nVHz^{-1}$ would yield the measured flux sensitivity of $3x10^{-6}\phi_o Hz^{-\frac{1}{2}}$. Thus, there is every reason to believe that substantial improvement in performance would result from proper impedance matching. However, this rather promising technique for junction fabrication appears not to have been pursued.

(vi) Microbridge dc SQUID with L=100pH Until very recently, it has not been possible to fabricate microbridges with a sufficiently high resistance to use them in SQUIDs with high sensitivity. However, Laibowitz et al. [20] have successfully fabricated Nb microbridges of extremely small dimensions, and these have been incorporated into SQUIDs [21]. The loop area is several μm^2, and the inductance is about 100pH. Each bridge is typically 30nm-thick, 50nm wide, and 300 to 1000nm long, with a resistance of about 40Ω and a critical current of typically 30μA at 4.2K. The energy sensitivity per Hz measured in an open loop configuration is typically ~3h at 4.2K, the highest sensitivity yet reported. Unfortunately, the critical current of these junctions increases as the temperature is lowered, and the I-V characteristics tend to become hysteretic so that the temperature dependence of the noise cannot be measured. From Eq.(11), we predict $\varepsilon/1Hz \approx 1.2x10^{-33} J\ Hz^{-1} \approx 1.8h$, somewhat less than the measured value. However, it should be noted that the onset of hysteresis when the critical current is increased by cooling the device suggests that self-heating in these microbriges may be severe, and that their actual temperature may be above the bath temperature.

To my knowledge, this is the first time that microbridges have been used to obtain very high sensitivity SQUIDs. Although the reliability of these devices has yet to be established, the strong temperature dependence of the

critical current may be a problem in certain applications, and the small loop area and possibly high kinetic inductance of the bridges may make coupling of external coils to the SQUID rather inefficient, nevertheless, the intrinsic performance is obviously very impressive. It is to be hoped that there will be considerable further work along these lines in the near future.

D. Discussion on DC SQUIDs

It appears from Table I that Eq. (11) tends to consistently underestimate the noise energy by a factor of 2 or 3. This discrepancy may be due to the neglect of the junction capacitance in the noise computation. In practice, one sometimes finds the measured values of S_V and V_ϕ are substantially higher than predicted, particularly in regions of high dynamic resistance, for example, near a self-resonant step. However, since both S_V and V_ϕ^2 tend to scale with the square of the dynamic resistance, their ratio may not be too far from the predicted value.

The use of thin films (as opposed to point contacts) now seems firmly established, and has clearly demonstrated the enormous benefits to be gained from photo- and electronlithography. However, it should be emphasized that none of the more sensitive devices has been operated in a flux-locked loop, an essential requirement for most applications since the dynamic range usually exceeds ϕ_0. Indeed, some of the SQUIDs, for example (iv), may well be rather less sensitive if flux-modulated in the usual way because the range of flux over which the best performance is obtained is so small. Furthermore, until recently, little attention has been paid to the problem of efficient coupling of planar SQUIDS to input coils.

The importance of coupling SQUIDs properly to the input circuit cannot be overestimated if optimum performance is to be obtained [13]. First, consider the relatively low frequency applications (up to a few hundred Hz) for which most SQUIDs are currently used. Because of the enormous physical size of the capacitors required and the inconvenience of a frequency-dependent response, the use of untuned circuits will probably continue. Since $T_N \propto \kappa^{-2}$ [Eq. (9)], one needs a reasonable value of κ, say 0.5. To match efficiently to most voltage sources or magnetometer pick-up loops at low frequencies one requires

input coils with inductances of 1μH or sometimes considerably more [13]. Good coupling to niobium wire coils of this size is straightforward with cylindrical SQUIDs, but notoriously difficult with planar geometries. One solution to this problem, of course, is to fabricate cylindrical SQUIDs with (say) $1\mu m^2$ junctions. However, this geometry is very inconvenient for lithographic processing. Recently, Ketchen and Jaycocks [22] have fabricated a planar SQUID with an inductance of about 0.1nH coupled to a 10-turn thin-film coil. The coil exactly overlays the SQUID loop, but is separated from it by a thin insulating film. This configuration gives very efficient coupling: In preliminary measurements, Ketchen and Jaycocks reported $\kappa = 0.6$ for a 12nH input coil. It is reasonable to expect that this technique can be extended to achieve relatively efficient coupling to coils with much higher inductances, possibly using a thin-film flux transformer. These developments are crucial if one is to take advantage of the great improvements in sensitivity of the devices themselves. Furthermore, the modification of the characteristics of the SQUID, and the effect of the highly non-linear SQUID inductance on the input impedance of the coil should be studied in detail.

For higher frequency applications (above say, 1kHz) where one may be interested in a relatively narrow signal bandwidth, there are considerable advantages to be gained from tuning the input [13, 23]. T_N is independent of κ, and the necessity for tight coupling can be relaxed, provided one can still satisfy the optimization conditions on the various components [13]. One important example is the transducer in gravity wave detectors [24], where one is concerned with a very narrow bandwidth at an operating frequency of typically 1kHz. As one goes to higher frequencies, the use of a tuned input becomes increasingly attractive. The use of dc SQUID amplifiers at high frequencies deserves serious considera-

tion since, at its' present level of understanding, the theory predicts near-ideal performance up to any frequency that is small compared with the Josephson frequency 2eV/h. Since eventually one might hope to operate a SQUID at a bias voltage $\sim$ 1mV, corresponding to 500 GHz, the upper frequency limit might well approach 100 GHz. Needless to say, it will first be necessary to test the predictions of the theory very carefully. To my knowledge, there has been no experimental measurement of the circulating current noise in a dc SQUID, nor of its' correlation with the voltage noise. In addition, there remains the considerable problem of coupling high frequency signals into the SQUID.

Finally, a brief discussion of 1/f noise is in order. All of the sensitivities reported are at frequencies above the 1/f region. Now the thermal fluctuation model for 1/f noise in a shunted junction [25] predicts that the spectral density of the voltage noise is proportional to $(dI_o/dT)^2 (\partial V/\partial I_o)_I^2 T^2/Ac_v$, where A is the junction area and c_v is the heat capacity of a unit area of junction with a thickness equal to the sum of the coherence lengths of the two superconductors. One can adapt this result to estimate the spectral density of 1/f noise in a tunnel junction SQUID by dividing it by V_ϕ^2, noting that $(\partial V/\partial I_o)_I/V_\phi \sim L$, and setting $2LI_o=\phi_o$. One finds $\varepsilon_{1/f}/1Hz$ to be proportional to $(dI_o/I_o dT)^2 T^2/LAc_v$. Thus, at a given temperature, $\varepsilon_{1/f}/1Hz$ is proportional to 1/LC, while for the white noise $\varepsilon/1Hz$ is proportional to $(LC)^{1/2}$. Evidently, as one reduces L and/or C to improve the white noise energy, the 1/f noise energy is expected to increase substantially. Preliminary measurements [26] of the 1/f noise in the low inductance SQUID (iv) indicate that the frequency at which 1/f noise appears does indeed increase roughly as predicted. Clearly, a thorough investigation of low frequency noise is urgently required, both for tunnel junction devices and for microbridge devices for which the 1/f model may or may not apply. It may well turn out that for low frequency applications one must trade off the white noise and 1/f noise contributions to obtain the optimum sensitivity.

III. RF SQUID

A. Principles of Operation

The rf SQUID consists of a single Josephson junction in a superconducting loop of inductance L [Fig. 11(a)]. The junction is usually modeled as an ideal non-hysteretic shunted tunnel junction, although the majority of rf SQUIDs use a point contact. Most SQUIDS are operated in the hysteric mode with I_0 chosen so that $LI_0 \approx \phi_0$. The SQUID is inductively coupled to the inductor of a resonant LC- circuit [Fig. 11(a)] excited at its' resonant frequency, typically 20 MHz to 10 GHz, by an rf current (at the higher frequencies, the tank circuit may be replaced with a microwave resonator). When the flux through the SQUID is $n\phi_0$, the V_{rf}-I_{rf} characteristic consists of a series of steps and risers, as indicated in Fig. 11(b) (I_{rf} and V_{rf} are the peak amplitudes of the rf current and voltage across the tank circuit). When the flux is changed each step splits; the characteristic at $(n+\frac{1}{2})\phi_0$ is also shown in Fig. 11(b). At an appropriate value of I_{rf}, V_{rf} oscillates as a function of ϕ with period ϕ_0 [Fig. 11(c)].

The circuitry used to flux-lock the SQUID is shown in Fig. 12. The rf voltage is amplified and rectified or, in some circuits, lock-in detected. Thus, a small change in ϕ produces a small change in the voltage at the output of the detector. A relatively low frequency ac flux (say, 50 kHz) with peak-to-peak amplitude $\phi_0/2$ is applied to the SQUID, and produces an ac voltage at the output of the rf detector. This signal is lock-in detected, amplified, and fed back to flux-lock the SQUID.

B. Noise and Optimization

Kurkijärvi [27] and Kurkijärvi and Webb [28] first calculated the intrinsic noise in the rf SQUID. The noise arises from the thermally-induced uncertainty in the value of flux at which the SQUID makes transitions between

adjacent quantum states. The spectral density of the intrinsic equivalent flux noise was found to be

$$S_\phi^{(i)} \simeq 1.3 \frac{(LI_o)^2}{\omega_{rf}} \left(\frac{2\pi k_B T}{I_o \phi_o}\right)^{4/3}, \tag{13}$$

provided the rf frequency, $\omega_{rf}/2\pi$, is less than $10^7(R/1\Omega)$Hz. The presence of the noise also tilts the steps in the $I_{rf} - V_{rf}$ characteristic [Fig. 11(b)]. If one defines α as the ratio of the voltage rise along a step to the voltage separation of successive steps, it can be shown that α is related to $S_\phi^{(i)}$ via the relation [29 - 31]

$$\alpha^2 = \omega_{rf} S_\phi^{(i)} / \pi \phi_o^2. \tag{14}$$

Jackel and Buhrman [29] reported that although α may exceed the value predicted by Eqs. (13) and (14) by as much as a factor of 5, nevertheless if one measures α, $S_\phi^{(i)}$ is accurately predicted from the measured value of α by Eq. (14).

When the SQUID is coupled via a tank circuit to an amplifier, these components contribute additional noise sources [29,32,33]. The overall noise referred to the input of the amplifier enables one to calculate the equivalent flux noise of an isolated SQUID. However, as in the case of the dc SQUID, when an input circuit is coupled to the rf SQUID, a more detailed analysis is required to optimize properly the noise temperature of the complete system. Ehnholm [30] derived an equivalent circuit of the rf SQUID, coupled to an input circuit and a tank circuit, that consists of a current amplifier with noise sources at the input and output. This model contains the important result that amplifier and tank circuit current noise is coupled through the non-linear inductance of the SQUID to appear as a voltage noise source in the input circuit. Thus, the input voltage noise is dominated by downconverted amplifier and tank circuit current noise coupled through the reverse transfer coefficient. (This

coefficient is essentially zero in the dc SQUID, since a noise introduced in the bias current does not couple to the input circuit, as least to first order [13].) Careful measurements of the reverse transfer coefficient [34,35] are in excellent agreement with the model. Measurements of the output noise by Ahola et al. [36] are also in good agreement with the model. More recently, Hollenhorst and Giffard [31] have presented an explicit calculation of the small-signal and noise parameters; their measurements of the input noise voltage are in very good accord with their predictions. These authors [35] show that the optimized noise temperature for a tuned input circuit can be written

$$T_N^{(opt)}(\omega) \simeq \frac{1}{4k_B}\left[(S_v^{(i)} + S_v)\, S_I\right]^{1/2} \frac{\omega}{\omega_{rf}} . \qquad (15)$$

In Eq. (15), $S_v^{(i)}$ is the spectral density of the voltage noise induced across the tank circuit by the intrinsic noise of the SQUID, while S_v and S_I are the spectral densities of the amplifier and tank circuit voltage and current noises, which are assumed to be uncorrelated.

Since few rf SQUIDS have been analyzed in sufficient detail to enable one to estimate $T_N^{(opt)}(\omega)$, we again characterize the noise energy by $\varepsilon/1\text{Hz}$ in order to compare different devices. For the rf SQUID, we must include preamplifier noise, which we characterize by the optimized noise temperature T_a obtained when the effective source impedance is equal to the ratio of the (uncorrelated) rms voltage and current noises. The preamplifier contribution to the energy sensitivity can be written as [29,33]

$$\frac{\varepsilon^{(a)}}{1\text{Hz}} = \frac{2\pi\alpha k_B T_a}{\omega_{rf}} . \qquad (16)$$

(As emphasized by Ahola et al. [36], an additional contribution arises when α is very small and/or an input circuit is strongly coupled to the SQUID. We will not consider this effect.) When the amplifier is at room temperature, some of the coaxial line coupling it to the tank circuit is at room temperature. Since the capacitance of the coaxial line and the amplifier are included in the resonant circuit, part of the tank circuit resistance is well above the bath temperature, and there will be a substantial contribution from the tank circuit noise that increases the effective noise temperature to $T_a^{(eff)}$. Values of $T_a^{(eff)}$ may be as high as 100K or more.

Adding $\varepsilon^{(i)}/1\text{Hz} = S_\phi^{(i)}/2L$ to $\varepsilon^{(a)}/1\text{Hz}$ we find

$$\frac{\varepsilon}{1\text{Hz}} = \frac{1}{\omega_{rf}}\left(\frac{\pi\alpha^2\phi_o^2}{2L} + 2\pi\alpha k_B T_a^{(eff)}\right) . \qquad (17)$$

Equation (17) demonstrates that the noise energy scales as $1/\omega_{rf}$. However, it must be borne in mind that the preamplifier noise temperature also tends to increase as ω_{rf} increases, so that at high frequencies the preamplifier noise may become dominant. In general, the relative importance of the two terms depends largely on whether the preamplifier is at room temperature, or is cooled to the bath temperature. Not only does T_a tend to decrease when the preamplifier is cooled, but also the contribution of the tank circuit becomes relatively insignificant. Notice that Eq. (17) actually depends on temperature because α is temperature dependent.

The following section describes a number of practical SQUIDS that illustrate how $\varepsilon/1\text{Hz}$ may be reduced by increasing ω_{rf} and/or decreasing $T_a^{(eff)}$.

B. Practical rf SQUIDs

The development of rf SQUIDs has followed a quite different course from the dc SQUIDs. Because the dc SQUID at He^4 temperatures is always dominated by its' intrinsic noise, efforts have been focused on improving the device itself.

In the case of rf SQUIDs, there has been relatively little development of the SQUIDs themselves, but a great deal of effort has been expended in improving the performance of the amplifiers at higher frequencies, and in reducing the tank circuit noise temperature.

(i) 20-30 MHz toroidal point contact SQUID The point contact toroidal rf SQUID [37] has been available commercially [38] for a number of years, and is undoubtedly by far the most widely used SQUID of any kind. The device is made from niobium in two sections that form a toroidal cavity when clamped together [Fig. 13(a)]. A niobium screw that is preset at room temperature forms the junction. The tank circuit inductor and signal coil are placed inside the toroidal cavity, or, in some designs in separate cavities, the latter configuration giving an extremely low cross-talk between the two coils. The toroidal design has several notable advantages: It is extremely rugged; it is self-shielding against ambient magnetic field fluctuations; and, although its' inductance is relatively low, it can be efficiently coupled to a signal coil with an inductance of 1μH or more. This SQUID is usually operated at either 20 or 30 MHz, and connected via a coaxial line to a room temperature amplifier with an FET input. Table II lists representative values of the appropriate parameters. The calculated energy sensitivity, $S_\phi/2\kappa^2 L$, is in good agreement with the measured value of about 5×10^{-29}JHz^{-1}.

(ii) 10 GHz thin film cylindrical SQUID In 1974, Pierce et al. [39] described an rf SQUID consisting of a thin film of an InSn alloy deposited on a 1.6 mm-dia hollow cylindrical substrate. A cut is made in the film to leave a bridge 1μm wide and 10 μm long. The device can be operated from 2K to 4.2K, and recycled in and out of liquid helium without degradation. The 10 GHz pump signal from a Gunn oscillator is connected to the SQUID via a cooled circulator to reduce the amount of high temperature thermal noise incident on the device, and the

reflected signal is coupled out through the circulator. The room temperature parametric amplifier has a noise temperature of about 200K. The measured energy sensitivity referred to input coils of between 50 and 600 nH is about 2×10^{-30} JHz^{-1} at frequencies above about 10 kHz; at lower frequencies, the spectral density of the noise increases as 1/f. Insufficient data were given to allow one to compare the measured performance with the theoretical sensitivity, but, in any case, the device was outside the region of validity of the thecry which would require $R>10^3\Omega$. Although the excessive 1/f noise makes the device somewhat unattractive for applications at low frequencies, this SQUID clearly demonstrated the substantial improvement that could be achieved with the use of microwave frequencies. However, the improvement is not as great as one might naively expect: The energy sensitivity is better than that of 20-MHz toroidal SQUID by a factor of 25, whereas if the sensitivity scaled as $1/\omega_{rf}$ one would expect an improvement of a factor of 500. A large part of the noise in the 10 GHz device is probably contributed by the amplifier.

(iii) and (iv) Tunnel Junction and Toroidal SQUIDs using cooled GaAs-FET amplifiers

GaAs-FETs work well when immersed in liquid helium at 4.2K, although the devices themselves are probably at a rather higher temperature because of resistive heating. Substantial reductions in noise temperature can be achieved, for example, to around 20K at 300 MHz, and 100K at 10 GHz. Gaerttner [40] appears to have been the first to use a cooled GaAs-FET with an rf SQUID, but unfortunately, he did not publish any details of his system. Ahola et al. [36] have described in detail the use of cooled GaAs-FETs as amplifiers for a thin-film SQUID with a Nb-NbOx-Pb tunnel junction at 60 MHz, and a point-contact toroidal SQUID at 200-500 MHz. The 60 MHz SQUID is coupled to a tank circuit in the usual way, while the toroidal SQUID has no tank circuit, but is coupled directly to the FET via a $\lambda/4$ transformer made of 20 Ω line. In these configurations, the tank circuit or transformer noise is negligible compared with

the intrinsic and amplifier noise contributions. In Table II, the relevant parameters for the 60 MHz thin-film device are listed. The noise temperature of the GaAs-FET is about 30K, including a 12K contribution from the following amplifier stage. With the SQUID at 4.2K, the overall value of

$S_\phi/2\kappa^2 L$ is 5×10^{-29} JHz.$^{-1}$ When the SQUID is cooled to ~0.1K in a dilution refrigerator, the intrinsic noise becomes negligible compared with the amplifier noise, and $S_\phi/2\kappa^2 L$ improves to 5×10^{-30} JHz.$^{-1}$ It should be remarked that κ is rather small, about 0.3: The energy sensitivities referred to the SQUID itself are about 5×10^{-30} JHz^{-1} and 5×10^{-31} JHz^{-1} for the device at 4.2K and 0.1K respectively.

Table II lists parameters for the toroidal SQUID at 200 and 400 MHz. The best performance achieved with the SQUID at 4.2K was about 5×10^{-30} JHz^{-1} referred to the input coil, in excellent agreement with the predicted value.

(v) and (vi) 430 MHz 2-hole point contact SQUID with cooled GaAs-FET and GaAs- Varactor diode amplifiers Long, Clark , Prance, and Richards [41] have described a 430 MHz SQUID that also uses a cooled GaAs-FET preamplifier. The SQUID is the two-hole version [2] shown in Fig. 13(b).

In contrast to Ahola et al. [36], these workers used a matched 50-Ω line to couple the tank circuit to the FET input. The parameters and performance of this system are shown in Table II. Subsequently, Long, Clark, and Prance [42] described an improved amplifier with a GaAs varactor diode that lowered the claimed noise temperature by more than a factor of 2. They do not quote a measured value of α: The value listed in Table II is that quoted in their earlier reference [41]. On that assumption, their measured energy sensitivity is a factor of about 20 better than predicted.

We note that the theory probably remains valid at 430 MHz: One requires $R \gtrsim 50\Omega$, a restriction that is likely to be satisfied by a point contact with a critical current of (say) 4μA. Since the earlier device (v) was already limited by intrinsic noise, it is a little difficult to understand how a reduction in the amplifier noise temperature can produce such a large improvement in the overall sensitivity. Even if one neglects the amplifier noise, one would require $\alpha \approx 0.1$ to produce the measured sensitivity, a value that seems to be appreciably less than values quoted in the literature. Thus, although the quoted sensitivity is excellent, the best obtained for rf SQUIDs, we must await clarification of the discrepancies between the measured performance and that expected theoretically.

(vii) 9 GHz point contact SQUID Hollenhorst and Giffard [44] have described a novel point contact rf SQUID operated at 9 GHz. The device, shown in Fig. 14, consists of a toroidal re-entrant structure machined from niobium with an axially mounted point-contact. A multiturn input coil is inserted in the toroidal cavity, and a modulation and feedback coil is mounted in a groove along one side of this cavity. Microwave signals are introduced from a 50 Ω line into a 22 Ω $\lambda/4$ matching section. The narrow annular gap between the point contact and the toroidal cavity has an electrical length of $\lambda/2$ and an impedance of 0.25 Ω to minimize coupling at 9 GHz.

The 9 GHz signal is fed into the SQUID via a cooled circulator to minimize the level of noise power coupled to the device. The reflected signal is coupled via the circulator to a 9 GHz synchronous receiver with a noise temperature of about 500K. The SQUID can then be incorporated into a feedback circuit in the usual way. The best energy sensitivity achieved was

$S_\phi/2\kappa^2L = 7\times10^{-31}JHz^{-1}$ at 2.7K. Since the theory is certainly invalid at 10GHz, no comparison of the sensitivity with the predictions of Eq. (17) can be made. However, the authors estimate that about 1/3 of the measured noise power was contributed by the amplifier. Thus, one would make only a relatively limited improvement by using a cooled amplifier with a lower noise temperature.

C. Discussion on rf SQUIDs

It is clear from Table II that by using higher pump frequencies and/or cooled amplifiers one can improve appreciably on the energy sensitivity of the 20 MHz toroidal SQUID coupled to a room temperature amplifier (i). Thus, working at 200 or 400 MHz and using a cooled GaAs-FET preamplifier, Ahola et al. (iv) improved $S_\phi/2\kappa^2L$ by an order of magnitude, and achieved good agreement with the sensitivity expected from the measured parameters of the device. Long et al. (v, vi) achieved even better performance , but there appear to be substantial discrepancies between their measured sensitivity and that predicted from the measured parameters: Particularly in the case of the system with the varactor diode, it would be very useful to know the measured value of α, and how the required low value (0.1) is achieved. A system operating at around 400 MHz with a cooled amplifier is not too expensive, and appears to be very practical for most applications.

When the frequency is increased to about 10 GHz, the signal available from the SQUID grows proportionately, but the sensitivity does not improve as much

as one might expect. Thus, Pierce et al. (ii) achieved a sensitivity of $2X10^{-30}JHz^{-1}$, comparable with the values achieved at 400 MHz with cooled pre-amplifiers, while Hollenhorst and Giffard (vii) achieved a sensitivity of $7X10^{-31}JHz^{-1}$. There seems to be relatively little chance of improving the sensitivity at X-band frequencies, and, in addition, these systems are expensive. However, it is possible that one may be able to improve the performance by working at somewhat lower frequencies. For example, if the toroidal device of Ahola et al. (iv) at 4.2K retained α=0.3 at 4 Ghz, and if one used a cooled amplifier with a noise temperature of 30K, one should be able to achieve a device limited largely by intrinsic noise with $S_\phi/2\kappa^2L\sim6x10^{-32}JHz^{-1}$. Another possible but somewhat restrictive approach is to cool the SQUID, thereby reducing α. For example, Ahola et al.[36] point out that if their SQUID (iv) were cooled to $\sim$0.1K, one might hope to achieve a sensitivity of close to $10^{-32}JHz^{-1}$. Further investigation of the frequency- and temperature-dependence of the sensitivity is clearly warranted.

Virtually nothing has been said about 1/f noise in this section. For a given device, as the pump frequency is raised, one expects the intrinsic 1/f noise to remain constant. Thus, if the white noise level is reduced, 1/f noise will become significant out to higher frequencies. Very little seems to be known about low frequency noise in point contact junctions or microbridges so that it is impossible to predict the effect of raising the junction resistance (to increase the allowed rf frequency) on the 1/f noise. If one uses a small area tunnel junction to operate at higher frequencies, it will contribute the same 1/f noise as it does for the dc SQUID.

IV. CONCLUDING REMARKS

The sensitivity of the dc SQUID has improved dramatically over the past year or so, from $\sim 2 \times 10^{-30}$ JHz^{-1} for the cylindrical tunnel junction SQUID (i) to $\sim 2 \times 10^{-33}$ JHz^{-1} for the planar microbridge SQUID (both values are referred to the SQUID itself). The performance of the devices is generally in good accord with theoretical predictions. It seems likely that a device operating at the quantum limit ($\varepsilon/1\text{Hz} \gtrsim \hbar$) will emerge soon. However, it must be emphasized that for practical applications it is essential to couple these recently developed planar devices efficiently to an input coil, and that the low inductance of some of them may make this a difficult problem. Poor coupling will result in substantial degradation of the sensitivity referred to the input coil. Furthermore, the most sensitive devices have not yet been operated in a flux-locked loop, and for most applications this is an essential requirement. Thus, problems of excess noise fed back from the room temperature circuitry may yet have to be tackled. It should also not be overlooked that the three most sensitive devices [(iii), (iv) and (vi)] have been produced in a laboratory with considerable resources, and relied on fabrication techniques that are not widely available at present. Nevertheless, the relative ease of reaching intrinsic sensitivities in the 10^{-31} - 10^{-32} JHz^{-1} range make the dc SQUID very attractive, and one might expect considerable effort to exploit them in practical circuits in the near future.

The sensitivity of the rf SQUID has also improved markedly over the past several years, by two orders of magnitude compared with the 20 MHz toroidal SQUID, but only by at most a factor of 5 compared with the 1974- 10 GHz SQUID of Pierce et al. [39]. These improvements have come about partly by using cooled preamplifiers, and partly by going to higher frequencies. Further improvements may be possible by cooling the SQUID to below 1K, although this severely limits the range of applications. Improvements may also still come

about by carefully choosing new operating frequencies. However, my general feeling is that it will be difficult and expensive to make substantial further improvements in sensitivity. I should like to stress, however, that the performances of the rf SQUIDS were measured relative to input coils, and, mostly, operated in feedback circuits. These important considerations should be borne in mind when comparing rf SQUIDs with their dc counterparts.

The question of 1/f noise appears to have been largely neglected in recent work. It is almost inevitable that as the white noise level of SQUIDs is reduced, 1/f noise will dominate up to higher frequencies. If the 1/f noise in tunnel junctions does scale inversely as the junction area, as is predicted by the present model, the spectral density of 1/f noise in both dc and rf SQUIDS will increase more rapidly than the spectral density of white noise ($\propto \text{area}^{-1/2}$) decreases. Thus, for optimum low frequency performance, one may have to compromise between the two types of noise. There appear to be no adequate models for 1/f noise in point contacts and microbridges. It is clear that a major effort to understand the origins of low frequency noise in SQUIDS is warranted.

Finally, to keep matters in perspective, one should realize that the highest possible sensitivity is necessary only for a very few exotic applications, for example, gravity wave detectors. For virtually all practical applications at frequencies below a few kHz, a device with a sensitivity of (say) 10^{-31}JHz^{-1}, properly coupled to an input circuit and operating in a flux-locked loop, is likely to be more than adequate. Questions of dynamic range, slewing rate, long term reliability, straightforward operation, and ease of changing input coils are then of greater concern than higher sensitivity.

ACKNOWLEDGMENTS

This work was supported by the Division of Materials Sciences, Office of Basic Energy Sciences, U. S. Department of Energy. I am grateful to Drs. T. D. Clark , M. B. Ketchen, and R. F. Voss for preprints of their work and for supplying unpublished information. I am grateful to Drs. M. B. Ketchen and R. F. Voss for Fig. 10, and to Dr. R. P. Giffard for Fig. 14. Finally, I am indebted to Drs. W. M. Goubau, R. Koch, D. J. Van Harlingen, and, particularly, R. P. Giffard, for their comments on the manuscript and for helpful dicussions.

REFERENCES

[1] R. C. Jaklevic, J. Lambe, A. H. Silver, and J. E. Mercereau, "Quantum interference effects in Josephson tunneling," Phys. Rev. Lett., vol. 12, pp. 159-160, 1964.

[2] J. E. Zimmerman, P. Thiene, and J. T. Harding, "Design and operation of stable rf-biased superconducting point-contact quantum devices, and a note on the properties of perfectly clean metal contacts,": J. Appl. Phys., vol. 41, pp. 1572-1580, 1970.

[3] J. E. Mercereau, "Superconducting magnetometers," Rev. Phys. Appl., vol. 5, pp. 13-20, 1970.

M. Nisenoff, "Superconducting magnetometers with sensitivities approaching 10^{-10}gauss," Rev. Phys. Appl., vol. 5, pp. 21-24, 1970.

[4] B. D. Josephson, "Possible new effects in superconductive tunneling," Phys. Lett., vol. 1, pp. 251-253, 1962.

[5] J. Clarke, "Low frequency applications of Superconducting QUantum Interference Devices," Proc. IEEE, vol. 61, pp. 8-19, 1973.

[6] J. Clarke, "Superconducting QUantum Interference Devices for low frequency measurements," in Superconductor Applications: SQUIDs and Machines, B. B. Schwartz and S. Foner, Eds., New York: Plenum Publishing Corporation, 1977, pp. 67-124.

[7] W. C. Stewart, "Current-voltage characteristics of Josephson junctions," Appl. Phys. Lett., vol. 12, pp. 277-280, 1968.

D. E. McCumber, "Effect of ac impedance on dc voltage-current characteristics of superconductor weak-link junctions," J. Appl. Phys., vol. 39, pp. 3113-3118, 1968.

[8] J. Clarke, W. M. Goubau, and M. B. Ketchen, "Tunnel junction dc SQUID: Fabrication, Operation, and Performance," J. Low Temp. Phys., vol. 25, pp. 99-144, 1976.

[9] M. B. Ketchen, W. M. Goubau, J. Clarke, and G. B. Donaldson, "Superconducting thin-film gradiometer," J. Appl. Phys., vol. 49, pp. 4111-4116, 1978.

[10] C. D. Tesche and J. Clarke, "DC SQUID: Noise and Optimization," J. Low Temp. Phys., vol. 29, pp. 301-331, 1977.

[11] R. F. Voss (private communication) has computed the noise with $\beta_c \neq 0$, and found a marked increase in the spectral density of the noise for $\beta_c > 0.5$. Thus, it may be necessary to limit β_c to 0.5 rather than to 1 to obtain optimum performance.

[12] C. D. Tesche and J. Clarke, "DC SQUID: Current Noise," J. Low Temp. Phys., vol. 37, pp. 397-403, 1979.

[13] J. Clarke, C. D. Tesche, and R. P. Giffard, "Optimization of dc SQUID Voltmeter and Magnetometer Circuits," J. Low Temp. Phys., vol. 37, pp. 405-420 (1979).

[14] R. Koch, D. J. Van Harlingen, and J. Clarke (unpublished).

[15] R. Koch and J. Clarke, "Small area tunnel junction dc SQUID," Bull. Am. Phys. Soc., vol. 24, p. 264, 1979; and to be published with D. J. Van Harlingen.

[16] R. F. Voss, R. B. Laibowitz, S. I. Raider, and J. Clarke, "All Nb low noise SQUID with 1μm tunnel junctions, J. Appl. Phys. , vol. 51, pp. 2,306-2309 (1980).

[17] M. B. Ketchen and R. F. Voss, "An ultra-low noise tunnel junction dc SQUID," Appl. Phys. Lett., vol. 35, pp. 812-815, 1979.

[18] J. H. Greiner, C. J. Kircher, S. P. Klepner, S. K. Lahiri, A. J. Warnecke, S. Basavaiah, E. T. Yen, John M. Baker, P. R. Brosious, H.-C.W. Huang, M. Murakami, and I. Ames, "Fabrication process for Josephson integrated circuits," IBM J. Res. and Dev., vol. 24 , pp. 195-205, 1980.

[19] E. L. Hu, L. D. Jackel, R. W. Epworth, and L. A. Fetter, "Experiments on Ge-Sn Barrier Josephson Junctions," IEEE Trans. Magn., vol. MAG-15, pp. 585-588, 1979.

[20] R. B. Laibowitz, A. N. Broers, J. T. C. Yeh, and J. M. Viggiano, "Josephson effect in Nb nanobridges," Appl. Phys. Lett., vol. 35, pp. 891-893, 1979.

[21] R. F. Voss, R. B. Laibowitz, and A.N. Broers, private communication.

[22] M. B. Ketchen and J. Jaycocks, unpublished.

[23] M. B. Simmonds, W. A. Fertig, and R. P. Giffard, "Performance of a resonant input SQUID amplifier system," IEEE Trans. Magn., vol. MAG-15, pp. 478 481, 1979.

[24] See, for example, S. P. Boughn, W. M. Fairbank, R. P. Giffard, J. N. Hollenhorst, M. S. McAshan, H. J. Paik, and R. C. Taber, "Cryogenic approach to an optimal gravitational wave detector" in Proceedings of the Academia Nazionale Dei Lincei International Symposium on Experimental Gravitation, B. Bertotti, Ed., pp. 271-285, 1976.

[25] J. Clarke and G. Hawkins, "Flicker (1/f) noise in Josephson tunnel junctions," Phys. Rev., Vol.B14, pp. 2826-2831, 1976.

[26] M. B. Ketchen and C. C. Tsuei, "Low frequency noise in small area tunnel junction dc SQUIDS," paper presented at the Second International Conference on Superconducting Quantum Devices, Berlin, May 6-9, 1980; to be published in the proceedings.

[27] J. Kurkijärvi, "Intrinsic fluctuations in a superconducting ring closed with a Josephson junction," Phys. Rev., vol. 6B, pp. 832-835, 1972.

[28] J. Kurkijärvi and W. W. Webb, "Thermal noise in a superconducting flux detector," Proc. Applied Superconductivity Conf., Annapolis, Md., (IEEE, New York) pp. 581-587, 1972.

[29] L. D. Jackel and R. A. Buhrman, "Noise in the rf SQUID," J. Low Temp. Phys., vol. 19, pp. 201-246, 1975.

[30] G. J. Ehnholm, "Complete Linear Equivalent Circuit for the SQUID," in SQUID, Superconducting QUantum Interference Devices and their Applications, (Walter de Gruyter, Berlin), H. D. Hahlbohm and H. Lubbig, Eds., pp. 485-499, 1977; "Theory of the signal transfer and noise properties of the rf SQUID," J. Low Temp. Phys., vol. 29, pp. 1-27, 1977.

[31] H. N. Hollenhorst and R. P. Giffard, "Input noise in the hysteretic rf SQUID: Theory and Experiment," J. Appl. Phys. vol. 51, pp. 1,719-1,725 (1980).

[32] J. Kurkijärvi, "Noise in the superconducting flux detector," J. Appl. Phys., vol. 44, pp. 3729-3733, 1973.

[33] R. P. Giffard, J. C. Gallop, and B. W. Petley, "Applications of the Josephson effects," Prog. Quant. Electr., vol. 4, pp. 301-402, 1976.

[34] G. J. Ehnholm, S. T. Islander, P. Östman, and B. Rantala, "Measurements of SQUID equivalent circuit parameters," J. de Physique, vol. 39, colloque C6, pp. 1206-1207, 1978.

[35] R. P. Giffard and J. N. Hollenhorst, "Measurement of forward and reverse signal transfer coefficients for an rf-biased SQUID," Appl. Phys. Lett., vol. 32, pp. 767-769, 1978.

[36] H. Ahola, G. H. Ehnholm, B. Rantala, and P. Östman, "Cryogenic GaAs-FET amplifiers for SQUIDs, "J. de Physique, vol. 39, colloque C6, pp. 1184-1185, 1978; J. Low Temp. Phys., vol. 35, pp. 313-328, 1979.

[37] R. A. Kamper and J. E. Zimmerman, "Noise thermometry with the Josephson effect," J. Appl. Phys., vol. 42, pp. 132-136, 1971.

[38] S. H. E., San Diego, California, and United Scientific (formerly S.C.T.), Mountain View, California.

[39] J. M. Pierce, J. E. Opfer, and L. H. Rorden, "A broadband thin-film SQUID magnetometer pumped at 10 GHz," IEEE Trans. Magn., vol. MAG-10, pp. 599-602, 1974.

[40] M. R. Gaerttner, unpublished - reported at Int. Mag. Conf., Toronto, 1974.

[41] A. Long, T. D. Clark, R. J. Prance, and M. G. Richards, "High performance UHF SQUID magnetometer," Rev. Sci. Instr., vol. 50, pp. 1376-1381, 1979.

[42] A. P. Long, T. D. Clark, and R. J. Prance, "Varactor tuned ultrahigh frequency SQUID magnetometer," Rev. Sci. Instr., vol.51, pp. 8-13, 1980.

[43] Using $\kappa^2 = 0.16$ calculated from the parameters given in ref. [39], one finds $S_\phi/2\kappa^2 L \approx 4 \times 10^{-31} JHz^{-1}$, a factor of 2 larger than the value quoted.

[44] J. N. Hollenhorst and R. P. Giffard, "High Sensitivity Microwave SQUID," IEEE Trans. Magn., vol. MAG-15, pp. 474-477, 1979.

Table I. Representative characteristics of 6 dc SQUIDS. All quantities are measured except the calculated $S_\phi/2L$ which is obtained from Eq. (11). With the exception of (i), all values of $S_\phi/2L$ are measured open loop.

TYPE	Junction area (μm^2)	R (Ω)	L (nH)	T (K)	V_ϕ ($\mu V \phi_o^{-1}$)	$S_\phi^{1/2}$ ($\phi_o Hz^{-1/2}$)	---Measured $S_\phi/2L$---- ($10^{-30} JHz^{-1}$)	(h)	Calculated $S_\phi/2L$ ($10^{-30} JHz^{-1}$)
(i) Cylindrical tunnel junction [8]	10^4	0.8	1	4.2	1	3×10^{-5}	2	3,020	0.60
(ii) Planar tunnel junction [15]	10^2	7	1.2	4.2	7	1×10^{-5}	0.18	270	0.08
(iii) Planar tunnel junction [16]	1	30	1	4.2	50	3.4×10^{-6}	0.025	37	0.015
				1.6	100	2.3×10^{-6}	0.011	17	0.006
(iv) Planar tunnel junction [17]	10	2	0.0115	4.2	4,000	1.3×10^{-7}	0.003	5	0.0027
				1.8	7,000	1.3×10^{-7}	0.003	5	0.0011
(v) Planar GeSn barrier [19]		40	0.2	2.0	300	3×10^{-6}*	0.1*	151*	0.0011
(vi) Planar microbridge [21]		40	0.1	4.2	7,000	3×10^{-7}	0.002	3	0.0012

*Limited by amplifier noise

Table II. Representative characteristics of 7 rf SQUIDS. All quantities are measured except $\epsilon^{(i)}$, $\epsilon^{(a)}$, and ϵ, which are calculated from Eqs. (14), (16) and (17); $S_\phi/2L$ is measured in a flux-locked loop for (i), (v), and (vii), and in an open loop for the remainder.

TYPE	AMPLIFIER	$\omega_{rf}/2\pi$ (MHz)	L (nH)	T (K)	$T_a^{(eff)}$ (K)	α	κ^2	Measured: $S_\phi/2L$ (10^{-30}JHz^{-1})	Measured: $S_\phi/2\kappa^2L$ (10^{-30}JHz^{-1})	Calculated: $\epsilon^{(i)}/1$Hz (10^{-30}JHz^{-1})	Calculated: $\epsilon^{(a)}/1$Hz (10^{-30}JHz^{-1})	Calculated: $\epsilon/1$Hz$=S_\phi/2L$ (10^{-30}JHz^{-1})
(i) Toroidal point contact [37]	RT FET	20	0.8	4.2	60	0.33	0.3	15	50	7	14	21
(ii) Cylindrical thin film microbridge [39]	RT PARAMETRIC	10,000		2-4.2	200				2			
(iii) Thin-film tunnel junction [36]	cooled GaAs-FET	60	0.25	4.2	30	0.2	0.09	4.5	50	3	1.4	4.4
			0.25	~0.1	30		0.09	0.5	5	negligible		
(iv) Toroidal point contact [36]	cooled GaAs-FET	200	0.4	4.2	40	0.3	0.25	1.5	6	1.2	0.8	2.0
		400	0.4	4.2	70	0.3	0.25	1.3	5	0.6	0.7	1.3
(v) 2-hole point contact [41]	cooled GaAs-FET	430	0.5	4.2	13	0.5	0.16	0.4	3	1.2	0.2	1.4
(vi) 2-hole point contact [42]	cooled GaAs-varactor diode	430	0.5	4.2	5.5	0.5	0.16	0.07	0.4 [43]	1.2	0.1	1.3
(vii) Re-entrant toroidal point contact [44]	RT heterodyne	9,000	0.3	2.7	500		0.5	0.35	0.7			

Figure Captions

Fig. 1. (a) Configuration of dc SQUID; (b) current-voltage (I-V) characteristic with $\phi = n\phi_0$ and $(n+\frac{1}{2})\phi_0$; (c) V vs. ϕ at constant bias current.

Fig. 2. DC SQUID in flux-locked loop.

Fig. 3. Voltage across current-biased dc SQUID produced by ac flux modulation with $\phi = n\phi_0$ and $(n+\frac{1}{2})\phi_0$.

Fig. 4. SQUID voltmeter, (a) tuned input, (b) untuned input.

Fig. 5. Cylindrical dc SQUID (i): Junction area $\approx 10^4 \mu m^2$.

Fig. 6. Planar dc SQUID (ii): Junction area $\approx 10^2 \mu m^2$.

Fig. 7. Photograph of planar dc SQUID (iii): Junction area $\approx 1\ \mu m^2$. (a) Shows the complete device, while (b) shows an enlargement of the junctions; the upper two horizontal strips are the Pd_2Si shunts.

Fig. 8. I-V characteristics of dc SQUID (iii), each with applied flux of $n\phi_0$ (max. critical current) and $(n+\frac{1}{2})\phi_0$ (min. critical current).

Fig. 9. V, $dV/d\phi$, V_n, ϕ_n, and ε vs. applied flux for dc SQUID (iii) biased at 3.7 μA and at a temperature of 1.5K.

Fig. 10. Planar dc SQUID (iv) with 10 μm^2 junctions, and inductance of 11.5 pH.

Fig. 11. (a) Configuration of rf SQUID; (b) V_{rf} vs. I_{rf} characteristic of rf SQUID for $\phi = n\phi_0$ and $(n+\frac{1}{2})\phi_0$; (c) V_{rf} vs. ϕ at constant I_{rf}.

Fig. 12. RF SQUID in flux-locked loop.

Fig. 13. (a) Toroidal rf SQUID (i and iv); (b) two-hole rf SQUID (v and vi).

Fig. 14. Toroidal re-entrant rf SQUID (vii).

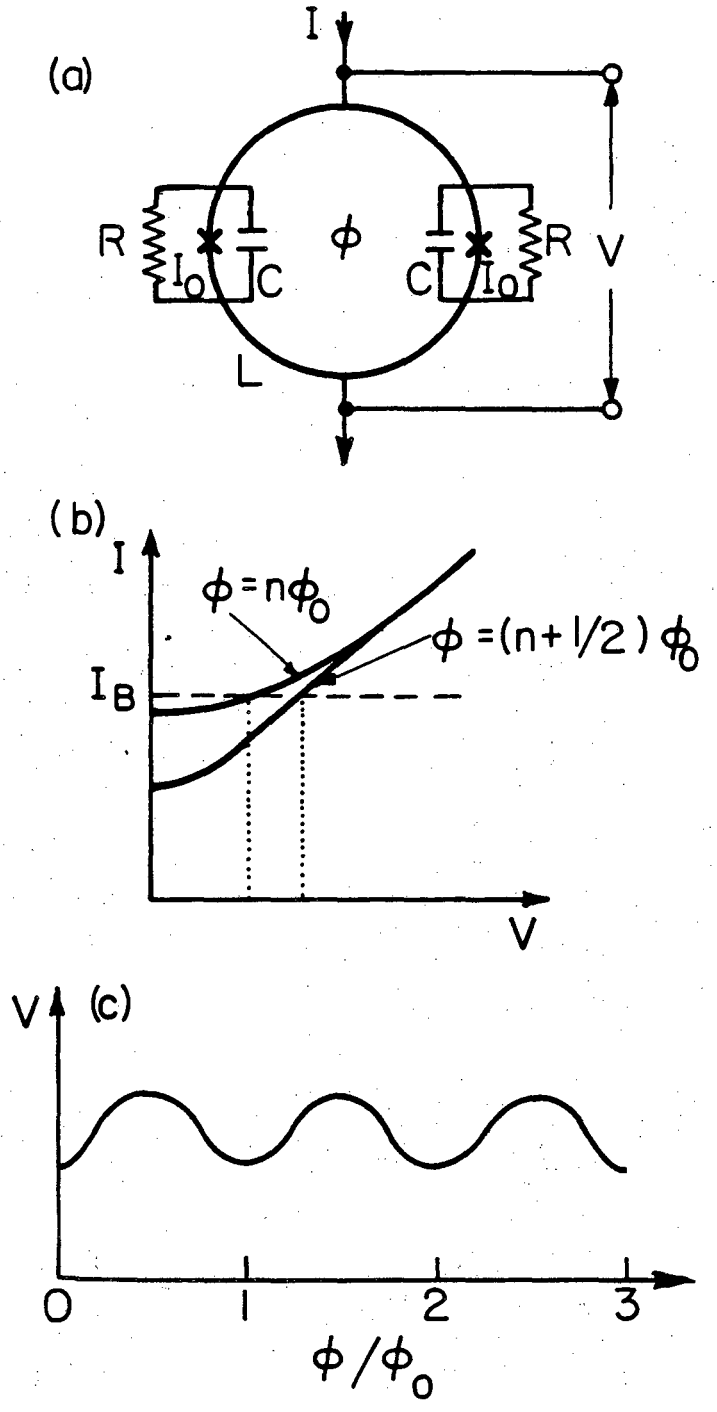

XBL 802-4740

Figure
1

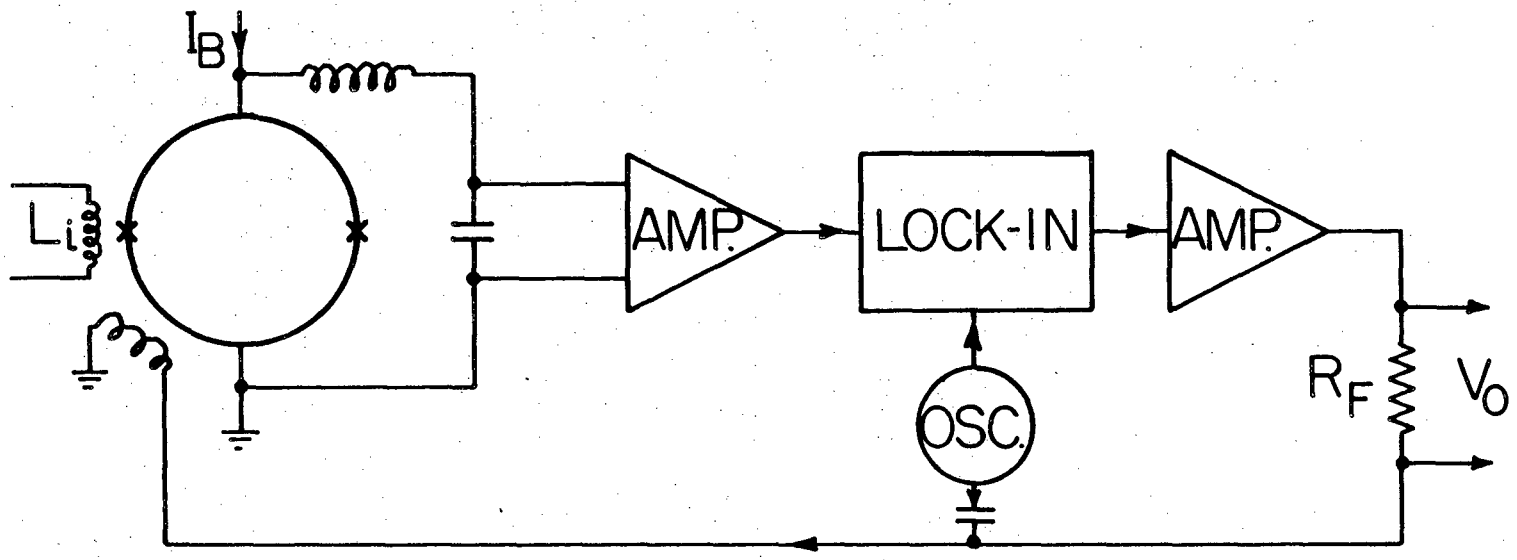

XBL802-4741

Figure
2

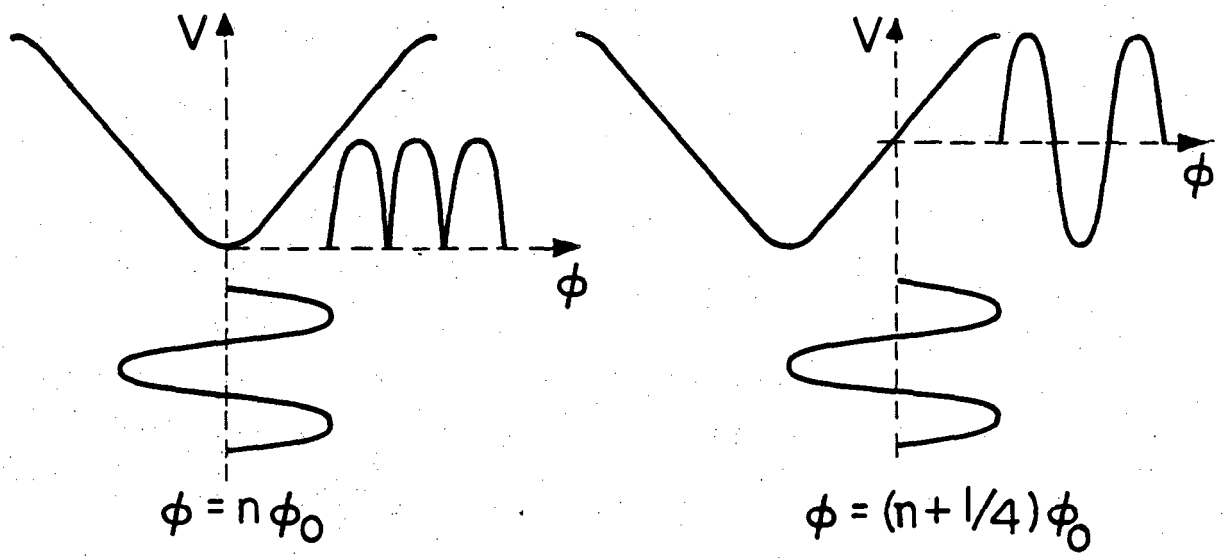

XBL 802-4739

Figure
3

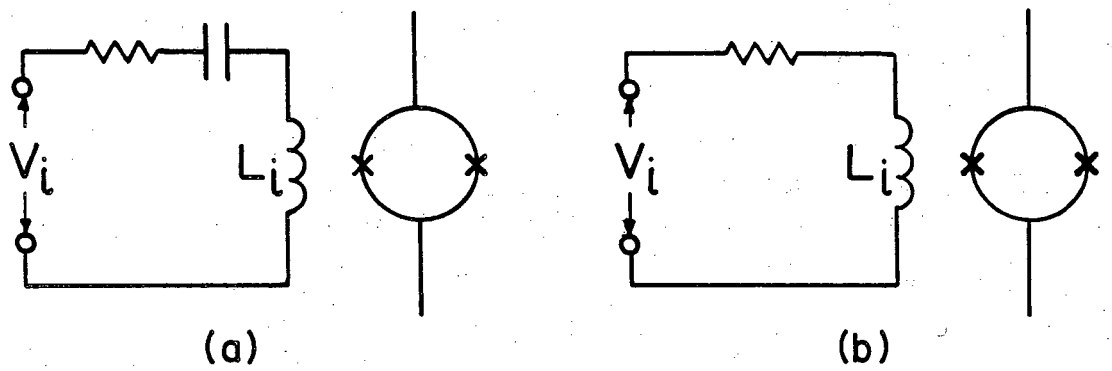

XBL 802-4738

Figure
4

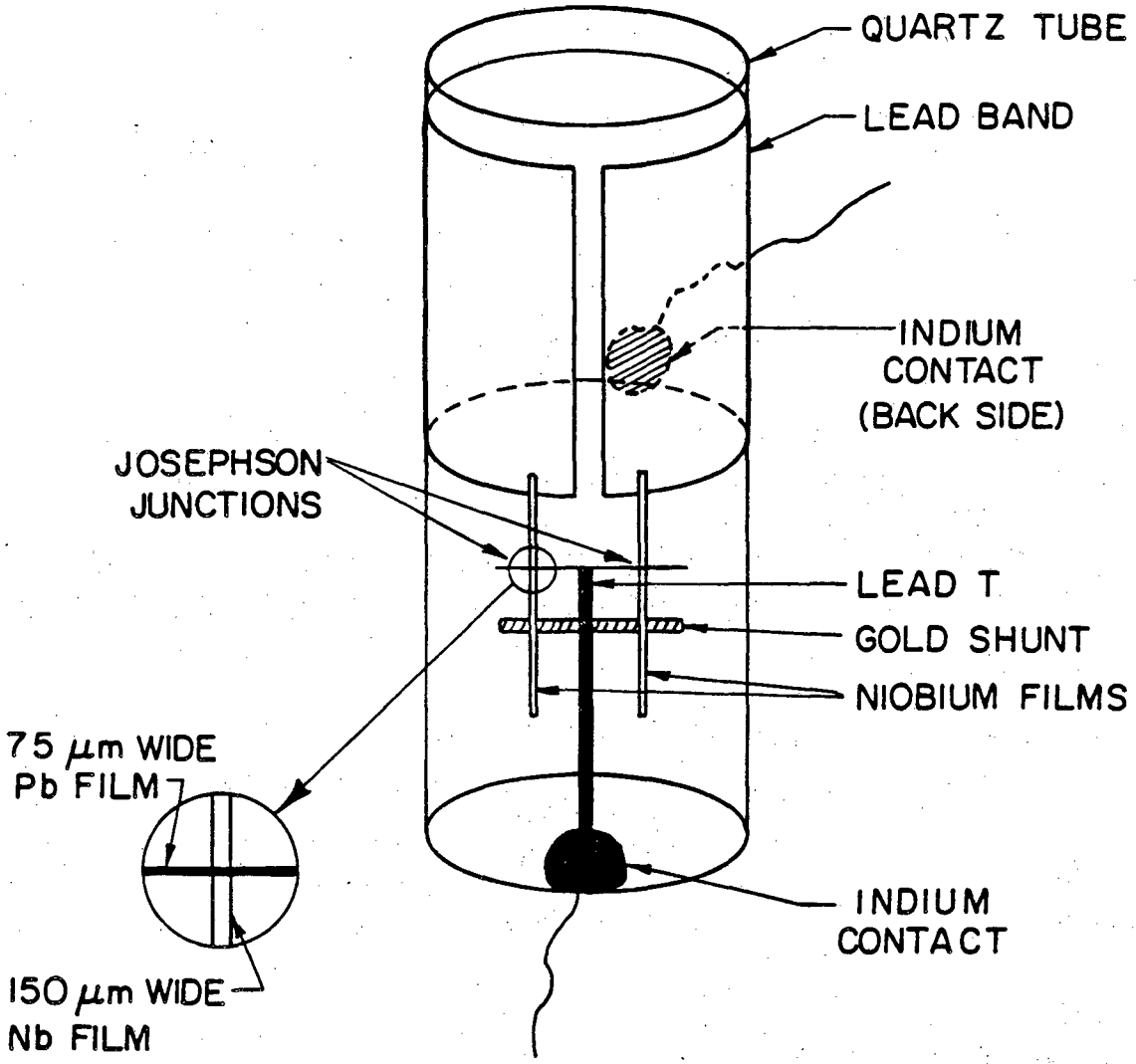
QUARTZ TUBE
LEAD BAND
INDIUM CONTACT (BACK SIDE)
JOSEPHSON JUNCTIONS
LEAD T
GOLD SHUNT
NIOBIUM FILMS
75 μm WIDE Pb FILM
150 μm WIDE Nb FILM
INDIUM CONTACT
XBL749-7211A

Figure
5

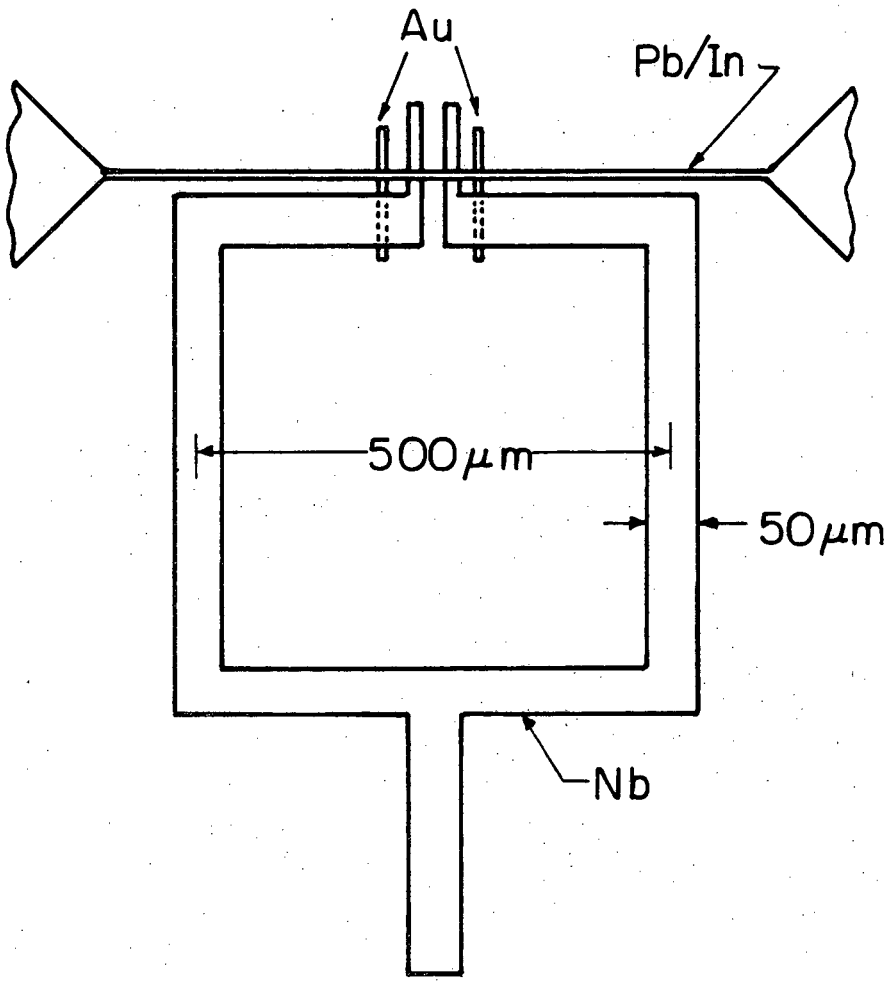

XBL 802-4742

Figure
6

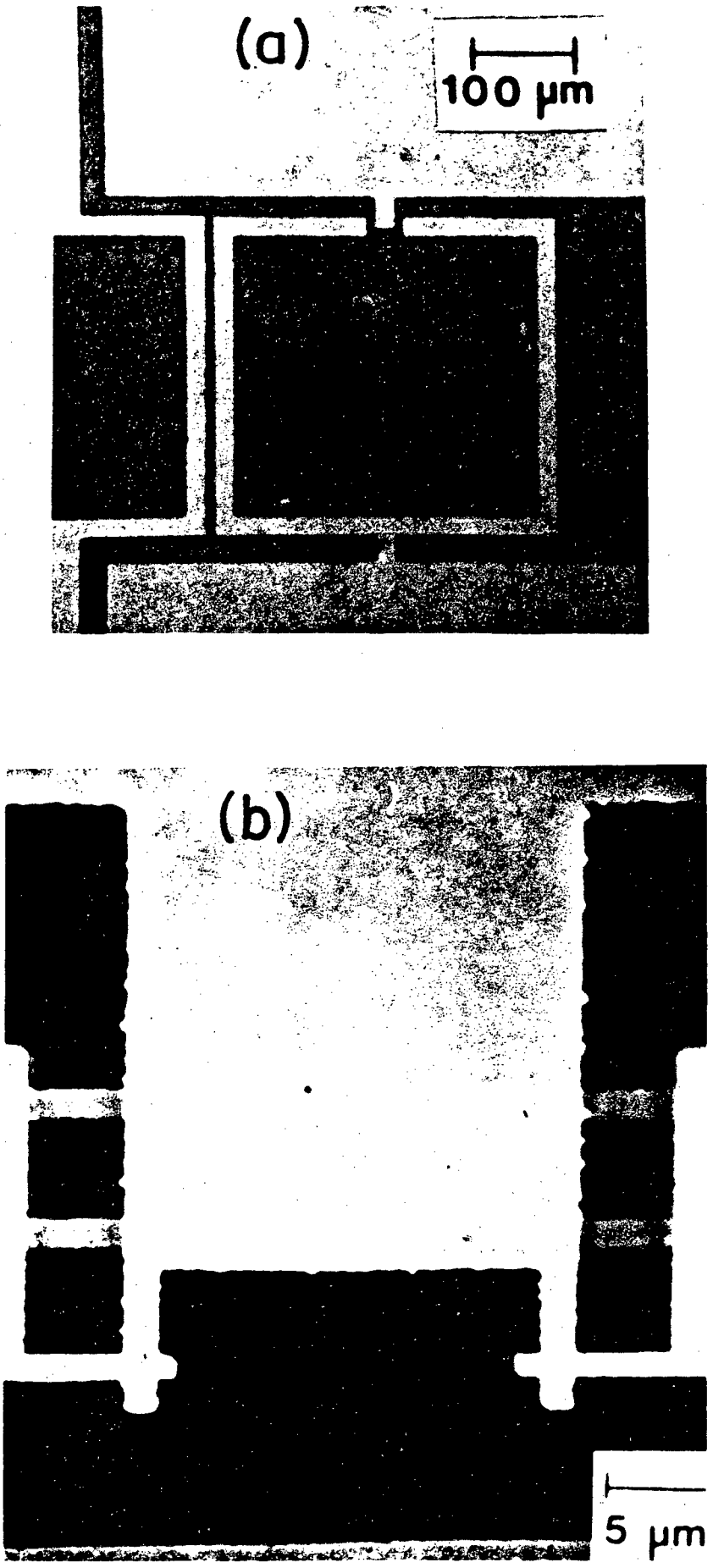

Figure
7

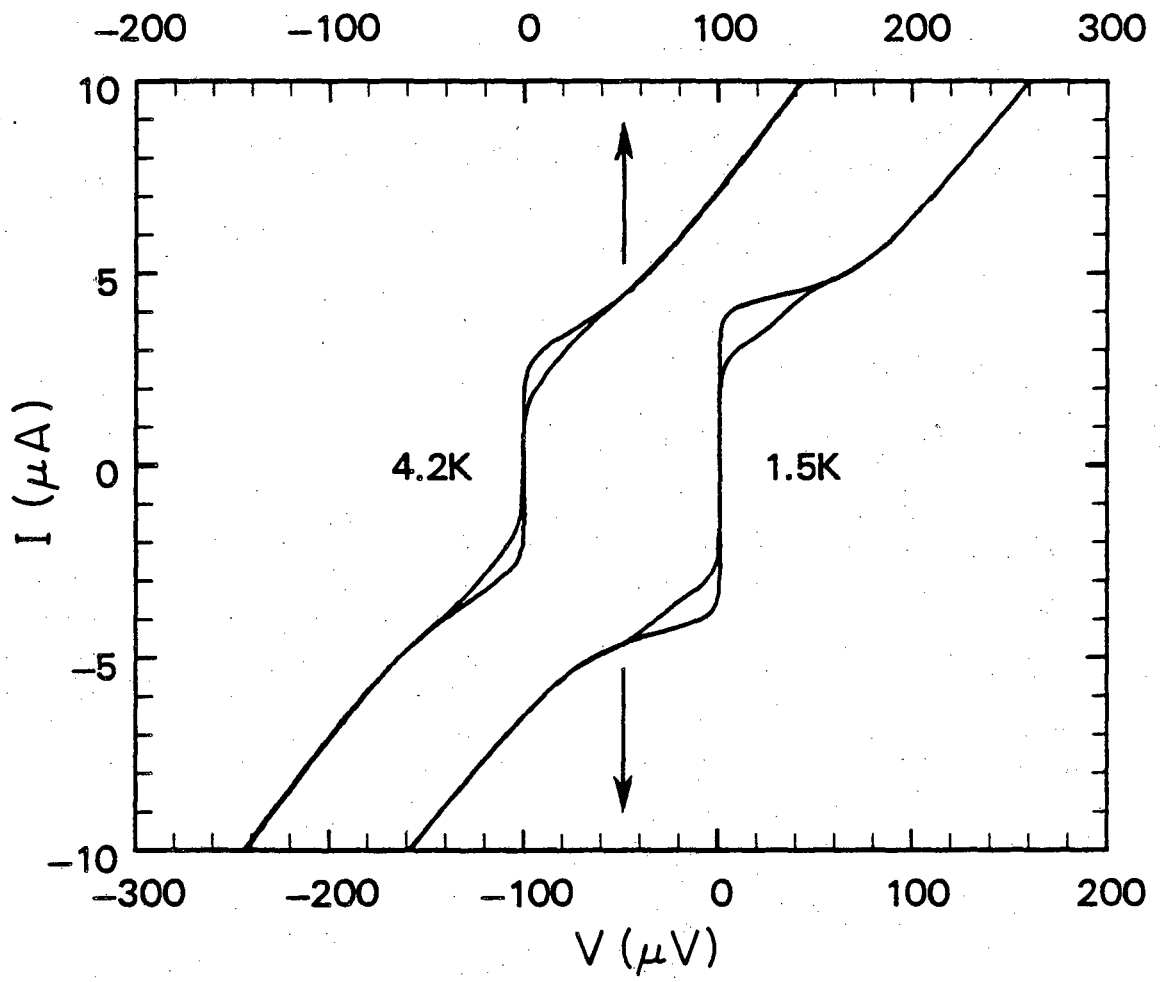
-200
-100
0
100
200
300
10
5
0
-5
-10
I (μA)
4.2K
1.5K
-300
-200
-100
0
100
200
V (μV)
XBL802-4736

Figure
8

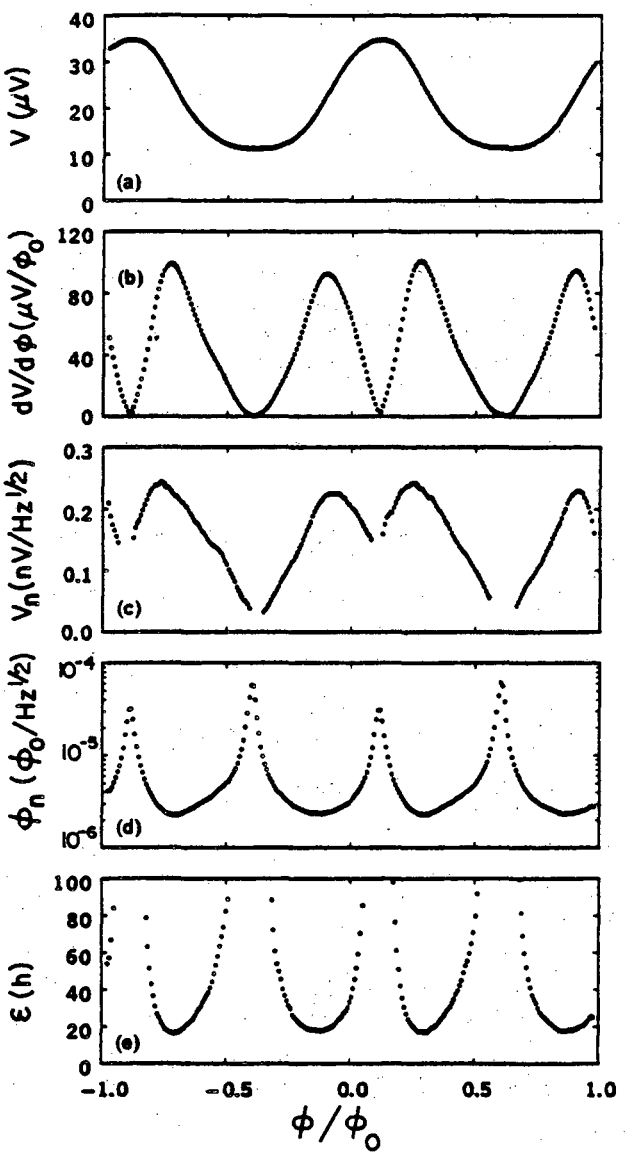

Figure
9

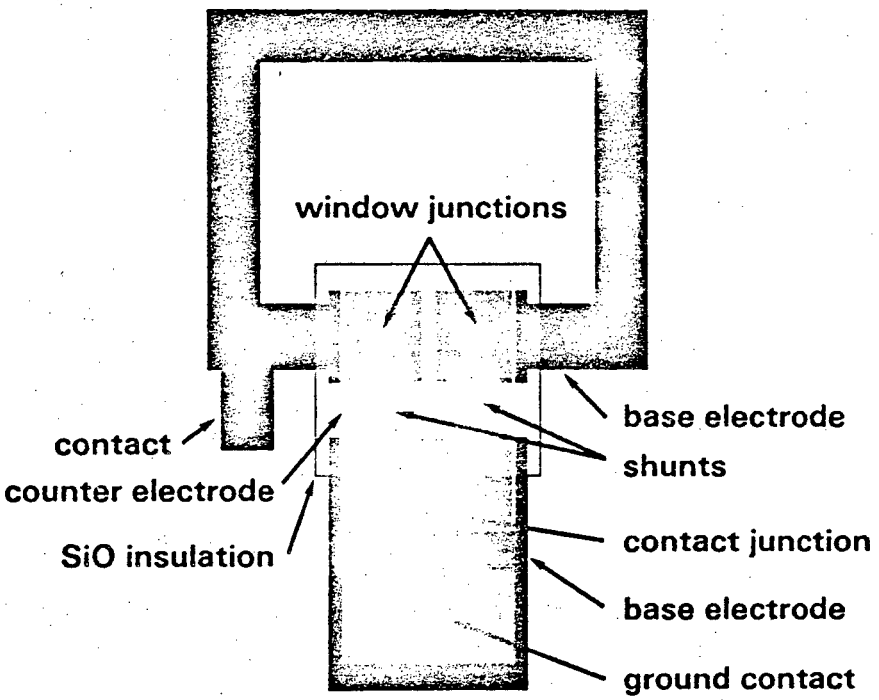
window junctions
contact
counter electrode
SiO insulation
base electrode
shunts
contact junction
base electrode
ground contact

Figure
10

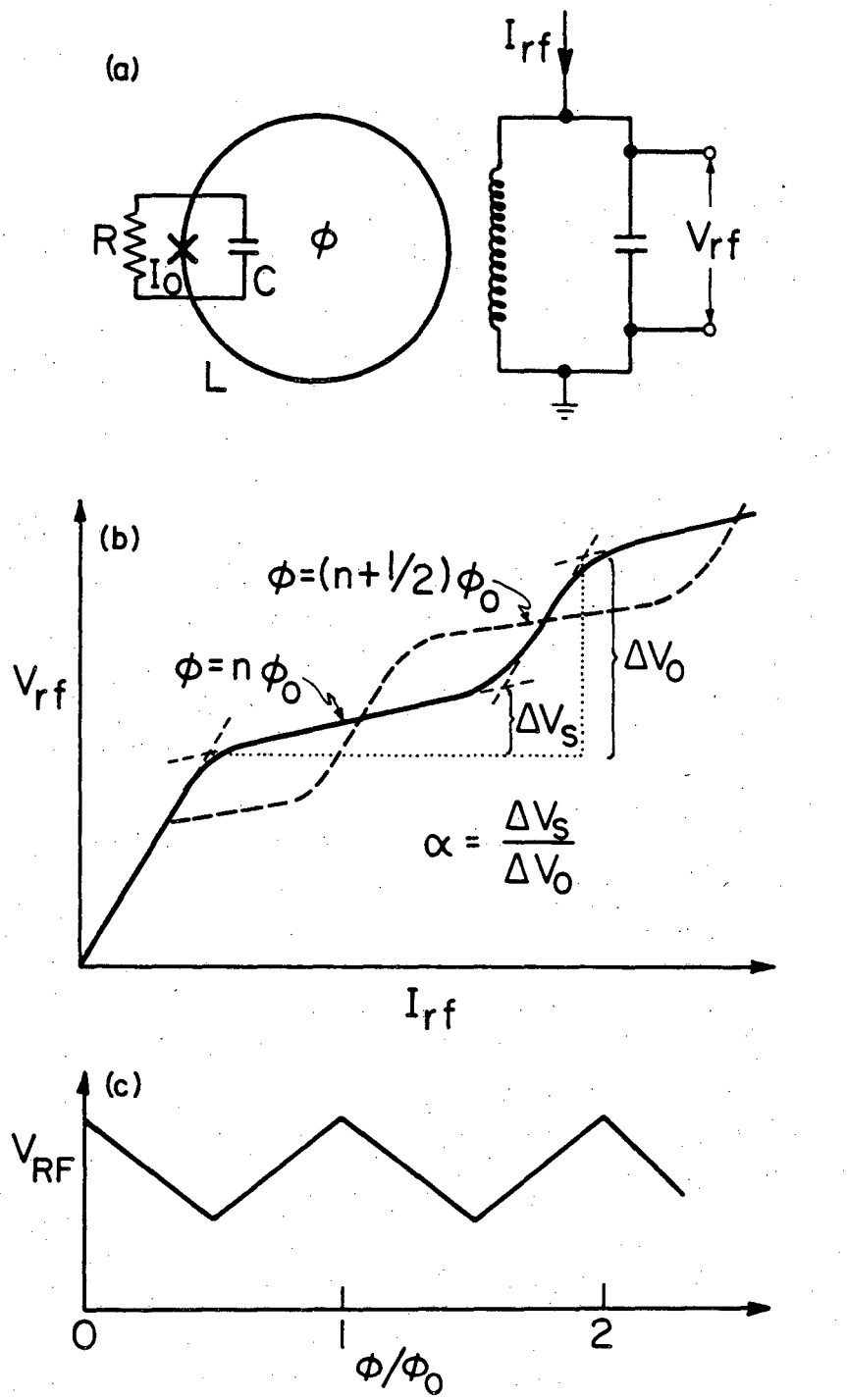

XBL802-4734

Figure
11

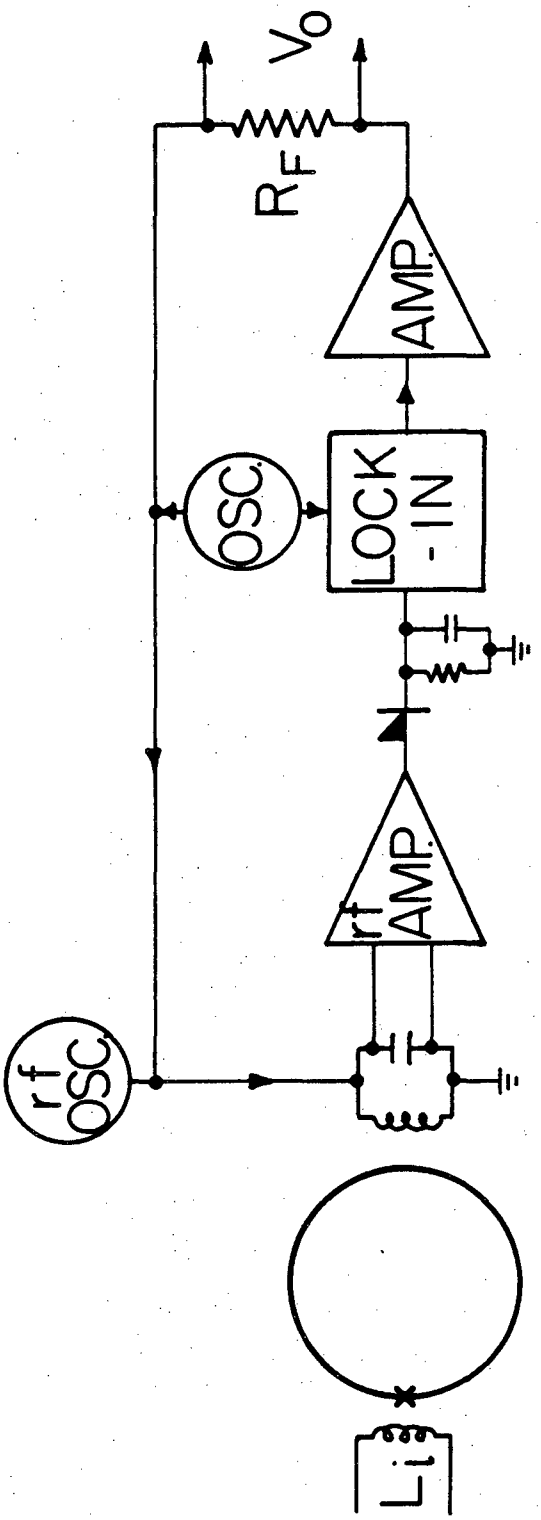

XBL802-4743

Figure
12

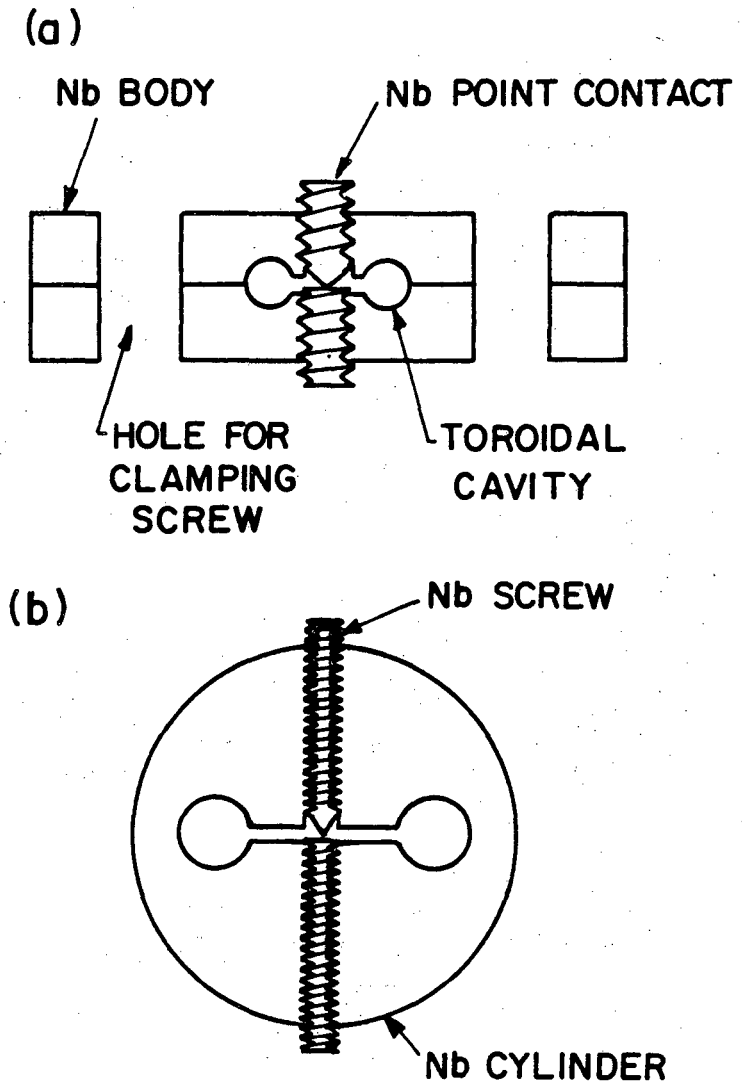
(a)
Nb BODY
Nb POINT CONTACT
HOLE FOR CLAMPING SCREW
TOROIDAL CAVITY
(b)
Nb SCREW
Nb CYLINDER
XBL 802-4737

Figure 13

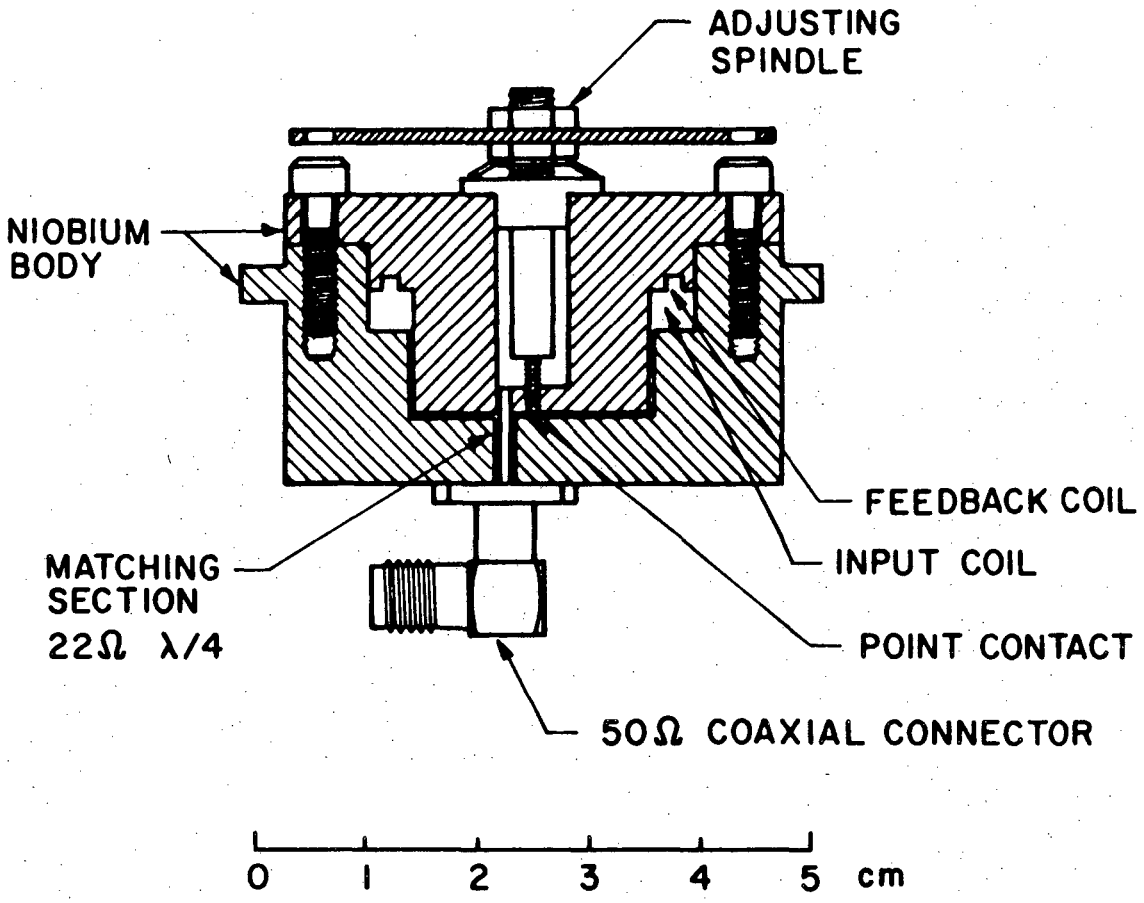
ADJUSTING
SPINDLE
NIOBIUM
BODY
FEEDBACK COIL
INPUT COIL
MATCHING
SECTION
22Ω λ/4
POINT CONTACT
50Ω COAXIAL CONNECTOR
0 1 2 3 4 5 cm
XBL 803-8663

Figure
14

TECHNICAL INFORMATION DEPARTMENT
LAWRENCE BERKELEY LABORATORY
UNIVERSITY OF CALIFORNIA
BERKELEY, CALIFORNIA 94720